Quaternary Research (2024), **119**, 65–85
doi:10.1017/qua.2023.63

Research Article

Glacier fluctuation chronology since the latest Pleistocene at Mount Rainier, Washington, USA

Mary Samolczyk[a*], Gerald Osborn[b], Brian Menounos[c], Douglas Clark[d], P. Thompson Davis[e], John J. Clague[f] and Johannes Koch[g]

[a]Earth Sciences, Yukon University, Whitehorse, Yukon, Canada; [b]Geoscience, University of Calgary, Calgary, Alberta, Canada; [c]Geography, Earth, and Environmental Sciences, University of Northern British Columbia, Prince George, British Columbia, Canada; [d]Geology, Western Washington University, Bellingham, Washington, USA; [e]Natural and Applied Sciences, Bentley University, Waltham, Massachusetts, USA; [f]Earth Sciences, Simon Fraser University, Burnaby, British Columbia, Canada and [g]Geography and Environment, Kwantlen Polytechnic University, Surrey, British Columbia, Canada

Abstract

Large stratovolcanoes in the Cascade Range have high equilibrium-line altitudes that support glaciers whose Holocene and latest Pleistocene advances are amenable to dating. Glacier advances produced datable stratigraphic sequences in lateral moraines, which complement dating of end moraines. New mapping of glacial deposits on Mount Rainier using LIDAR and field observations supports a single latest Pleistocene or early Holocene advance. Rainier R tephra overlies deposits from this advance and could be as old as >11.6 ka; the advance could be of Younger Dryas age. Radiocarbon ages on wood interbedded between tills in the lateral moraines of Nisqually, Carbon, and Emmons glaciers and the South Tahoma glacier forefield suggest glacier advances between 200 and 550 CE, correlative with the First Millennium Advance in western Canada, and during the Little Ice Age (LIA) beginning as early as 1300 CE.

These results resolve previous contradictory interpretations of Mount Rainier's glacial history and indicate that the original proposal of a single pre-Neoglacial cirque advance is correct, in contrast to a later interpretation of two advances of pre- and post-Younger Dryas age, respectively. Meanwhile, the occurrence of the pre-LIA Burroughs Mountain Advance, interpreted in previous work as occurring 3–2.5 ka, is questionable based on inherently ambiguous interpretations of tephra distribution.

Keywords: Glacier fluctuations, Lateral-moraine stratigraphy, Holocene, Mount Rainier, Environmental reconstruction, Little Ice Age

INTRODUCTION

The use of glacial sediments and landforms to reconstruct post-Wisconsinan alpine glacial histories is well established (e.g., Menounos et al., 2009). In the contiguous United States, the large stratovolcanoes of the Pacific Northwest are obvious places to study latest Pleistocene and Holocene glacier advances because of the relatively large volumes of glacier ice on the high peaks (Fig. 1). Indeed there has been much study of glacier activity on these volcanoes, but knowledge of the chronology of glacier advances is incomplete because dating has been based largely on end moraines, many of which were overridden during more extensive Little Ice Age (LIA) advances. Additionally, the timing of latest Pleistocene/Early Holocene advances and retreats remains contentious (e.g., Davis and Osborn, 1987; Thomas et al., 2000; Kovanen and Beget, 2005; Osborn et al., 2012). Kaufman et al. (2003) reviewed Cascade glacier chronologies and concluded that, depending on the author and the mountain the author studied, Younger Dryas glaciers (1) advanced a little, (2) advanced a lot, or (3) were in a state of retreat. They concluded that these disparities should be resolved with additional research.

Corresponding author Mary Samolczyk; Email msamolczyk@yukonu.ca

Cite this article: Samolczyk M, Osborn G, Menounos B, Clark D, Davis PT, Clague JJ, Koch J (2024). Glacier fluctuation chronology since the latest Pleistocene at Mount Rainier, Washington, USA. *Quaternary Research* **119**, 65–85. https://doi.org/10.1017/qua.2023.63

Mount Rainier and other Cascade volcanoes offer the advantage of having tephra-bearing sediments that can serve as stratigraphic markers (Mullineaux, 1974; Sisson and Vallance, 2009; Table 1). Rainier R tephra is a particularly useful marker for our study because it was deposited near the Holocene/Pleistocene boundary. Using R tephra along with dendrochronology, Crandell and Miller (1974) argued that there was an early Neoglacial advance on Mount Rainier, preceding LIA advances. They also established that glaciers advanced prior to the deposition of R tephra, which at that time was dated to >8.75 ka (Crandell et al., 1962). In contrast, Heine (1997, 1998a, b) radiocarbon-dated lake and bog cores near the heads of several valleys east of Mount Rainier and proposed two latest Pleistocene/Early Holocene advances on Mount Rainier—one shortly before the Younger Dryas and one afterwards.

Our study was initiated to test Heine's conclusions about pre-Neoglacial glacier activity on Mount Rainier and to resolve further the Neoglacial history. For the former goal, we employ high-resolution LIDAR and Google Earth imagery, field work, and a new lake sediment core. For the latter goal, we use lateral-moraine stratigraphy, which has been employed in the Canadian Cordillera for nearly four decades (e.g., Osborn, 1986; Ryder and Thomson, 1986), but only recently in the United States (Osborn et al., 2012).

The definitions of Neoglacial/Neoglaciation and LIA vary between studies and regions. In this paper we take

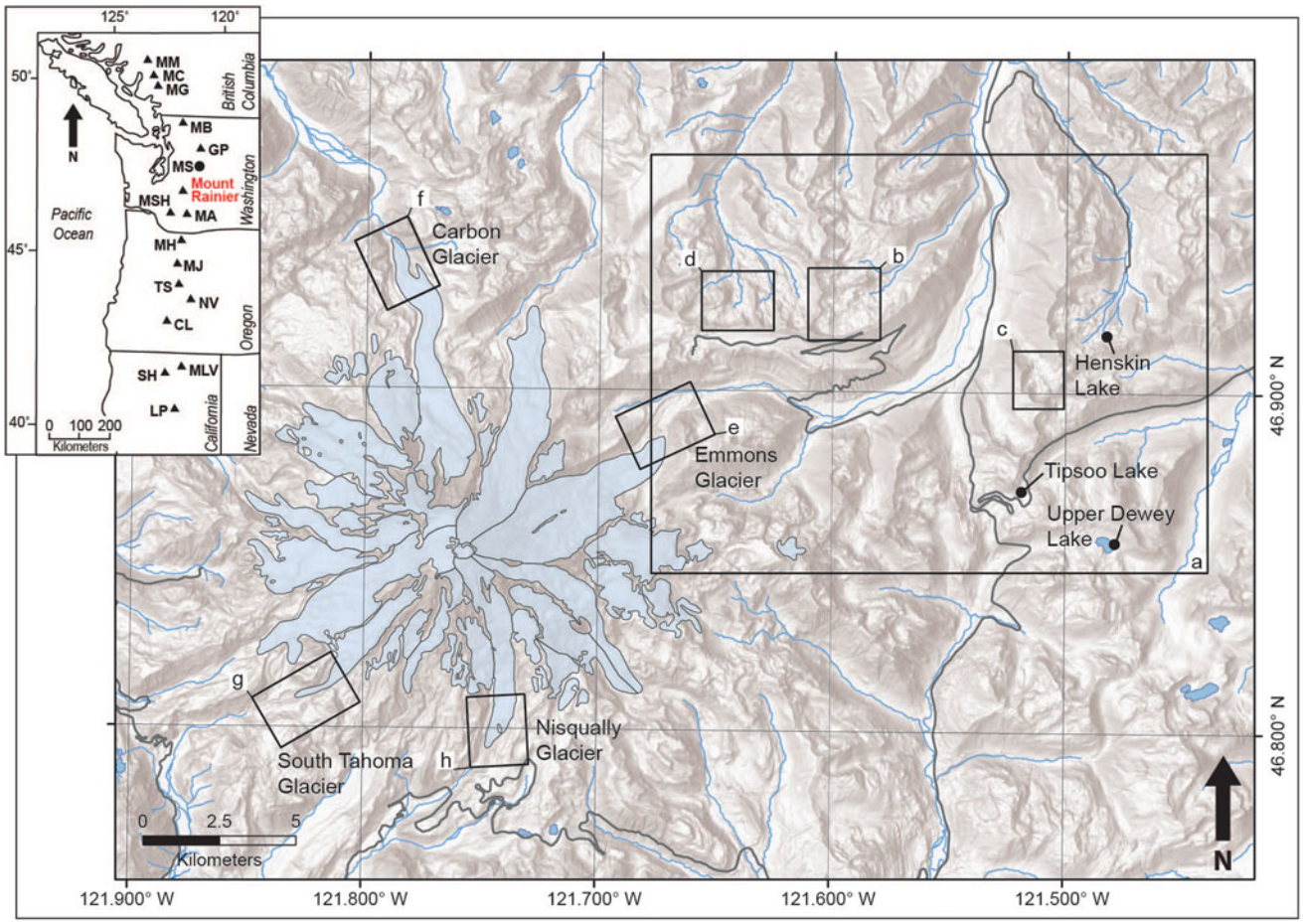

Figure 1. Map of Mount Rainier and surrounding area in Washington, U.S.A. Boxes with letters are study areas: a = Heine's (1998a, b) general study area; b = White River Park and Meadow X (see also Fig. 4); c = Crystal Lakes (see also Fig. 5); d = McNeeley type moraine location in Huckleberry Park (see also Fig. 2); e = Emmons Glacier and forefield (see also Fig. 7); f = Carbon Glacier and forefield (see also Fig. 8); g = South Tahoma Glacier and forefield (see also Fig. 9); h = Nisqually Glacier and forefield (see also Fig. 6). Key lakes discussed in this study are indicated and include Tipsoo, Henskin, and Upper Dewey lakes. Inset map shows the locations of notable volcanoes of the Cascade Volcanic Arc, including Mount Rainier (in red) and MM = Mount Meager, MC = Mount Cayley, MG = Mount Garibaldi, MB = Mount Baker, GP = Glacier Peak, MSH = Mount St. Helens, MA = Mount Adams, MH = Mount Hood, MJ = Mount Jefferson, TS = Three Sisters, NV = Newberry Volcano, CL = Crater Lake, MLV = Medicine Lake Volcano, SH = Mount Shasta, LP = Lassen Peak. Mount Stuart (MS) is a non-volcanic peak.

Neoglaciation to mean the climatic episode characterized by rebirth and/or growth of glaciers following maximum shrinkage during the Early Holocene warm interval (Porter and Denton, 1967). It may encompass the last few to last several millennia, depending on the region. For the beginning of the LIA we use the definition of Clague et al. (2009), about 1200 CE. The Younger Dryas cold interval, recorded as a period of glacier advance at the end of the Pleistocene, occurred between 12.9 and 11.7 ka before present, where present is 1950 CE (Davis et al., 2009; Cheng et al., 2020).

Table 1. Select tephra layers found in Mount Rainier National Park that are referenced in this study.

Tephra	Age (ka)	Source
W	0.471[a]	Mount St. Helens (Mullineaux, 1974; Yamaguchi, 1983; Fiacco et al., 1993)
C	2.2[a]	Mount Rainier (Mullineaux, 1974; Swanson, 1993)
Y	4.40–3.60[a]	Mount St. Helens (Mullineaux, 1974; Crandell et al., 1981; Sisson and Vallance, 2009)
O	7.777–7.477[b]	Mazama (Zdanowicz et al., 1999; Egan et al., 2015)
R	10.13–9.96[a]	Mount Rainier (Samolczyk et al., 2016)
R (new)	>11.6	Mount Rainier (this paper)

[a]Ages are in calibrated years before 1950.
[b]Age estimated from the GISP2 ice core (Zdanowicz et al., 1999).

Setting

Mount Rainier (4392 m asl) is the highest mountain of the Cascade Range (Rogers, 1985) (Fig. 1). Several periods of andesitic to dacitic volcanism since 500 ka have built the current edifice of the volcano (Fiske et al., 1963; Sisson and Lanphere, 2008). Surficial deposits on Mount Rainier comprise Holocene debris flows and fluvial, glacial, and pyroclastic deposits (Crandell, 1969).

Twenty-eight named glaciers extend partway down the flanks of the mountain and have a total area of about 75 km^2 as of 2021 (Beason et al., 2022). Additionally, the volcano is spotted with dozens of unnamed permanent ice patches and snowfields (Beason et al., 2022). The present retracted state of glaciers

https://doi.org/10.1017/qua.2023.63 Published online by Cambridge University Press

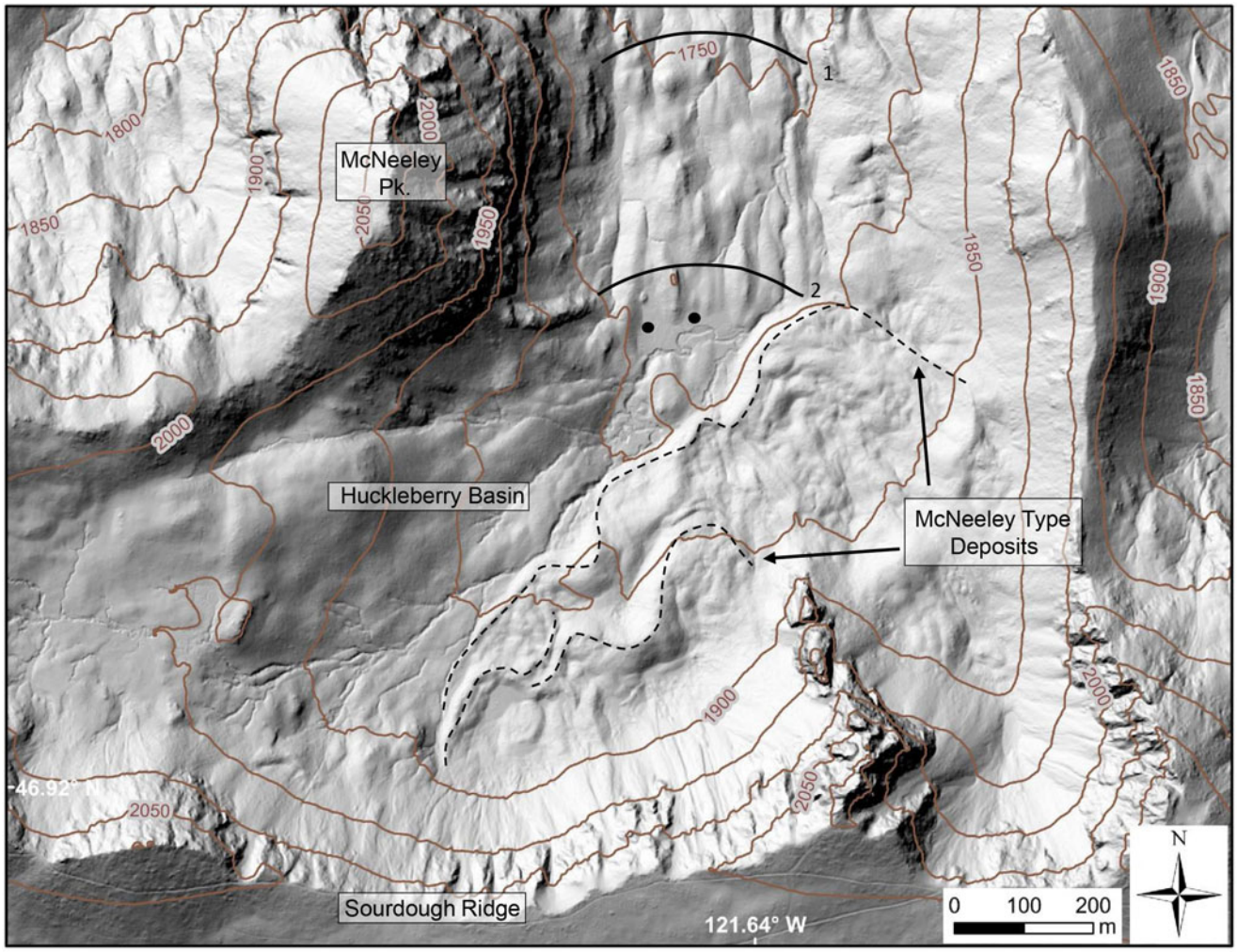

Figure 2. LIDAR image of the Huckleberry Park area. Dashed lines are moraine ridges. These features encompass the type McNeeley moraines first identified by Crandell (1969). Solid black curved lines are the locations of Heine's (1998a, b) McNeeley I and II moraines in the drainage. Solid black dots indicate Heine's (1998a, b) coring locations.

exposes extensive lateral-moraine complexes with proximal flanks sloping up to 60°, and to heights locally exceeding 100 m (Mills, 1978). Currently, glaciers on Mount Rainier have negative mass balances and are in a general state of retreat (Riedel and Larrabee, 2011). The seven-year average (2003–2009) equilibrium-line-altitude (ELA) of Nisqually Glacier was approximately 3160 m asl, and that of Emmons Glacier was 2730 m asl (Riedel and Larrabee, 2011). In comparison, the average ELA estimated from several glaciers during the farthest extent of LIA advances is about 1965 m asl (Burbank, 1981, 1982).

Mount Rainier and the surrounding region experience a Pacific Maritime climate. Winters are typically mild and wet because of westerly low-pressure systems, and summers are warm and dry from northerly high-pressure systems (Brace and Peterson, 1998). Strong orographic effects influence precipitation and temperature gradients on the volcano. Northeasterly flow during winter storms enhances precipitation on the western and southwestern flanks of the volcano and reduces precipitation on the opposite sides. For example, weather stations on the south and southeast flanks of the mountain at Paradise (1647 m asl; 46.786°N, −121.742°W) and Longmire (825 m asl; 46.749°N, −121.812°W) record mean annual precipitation of 3200 mm and 2210 mm, respectively, whereas a weather station at Ohanapecosh (560 m asl; 46.731°N, −121.571°W) on the east flank of the volcano records mean annual precipitation of 1905 mm (National Park Service, 2021a). Average high and low January temperatures at Paradise, Longmire, and Ohanapecosh are 0.5°/−6°C, 2°/−4°C, and 4°/−1°C, respectively. Corresponding average July highs and lows are 18°/7°C, 24°/8°C, and 23°/9°C, respectively (National Park Service, 2021b).

Previous work

Apart from older studies of recent glacial recession by Russell (1898), Matthes (1928), and Bender and Haines (1955), the first analysis of glacial history on Mt. Rainier was that of Sigafoos and Hendricks (1961), who conducted a tree-ring study of the recent history of Nisqually Glacier. Later, Sigafoos and Hendricks (1972) reported tree-ring ages for LIA moraines of eight glaciers on the mountain. Based on these studies, they reported evidence of advances terminating at about 1525, 1550, 1625–1660, 1715, 1730–1765, 1820–1860, 1875, and 1910 CE. These ages are from trees growing on moraines and thus are all minima.

https://doi.org/10.1017/qua.2023.63 Published online by Cambridge University Press

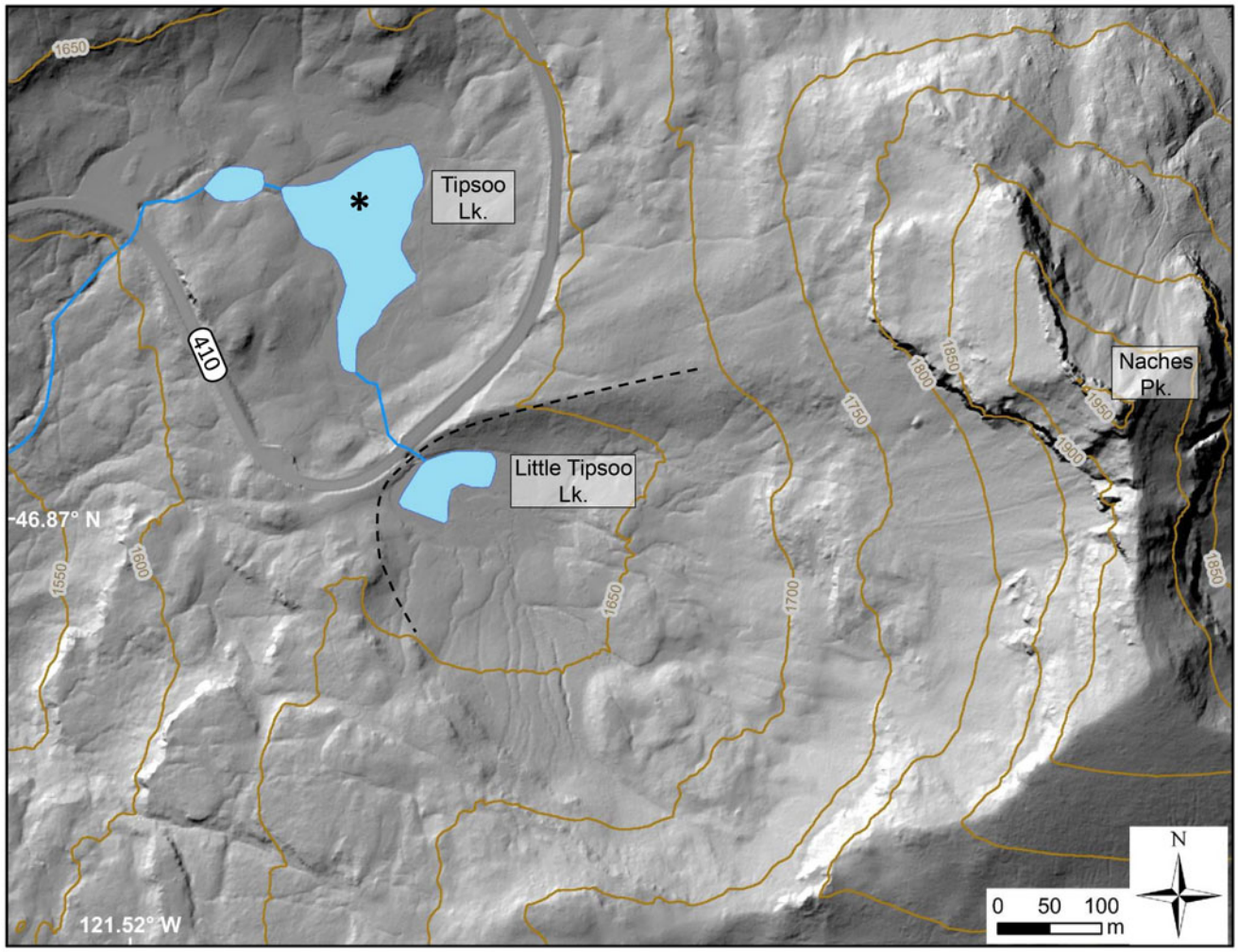

Figure 3. LIDAR image of Tipsoo Lake and cirque showing coring site (asterisk) and the crest of the McNeeley moraine (dashed line), first mapped by Crandell (1969) and supported by Heine (1998a, b). This moraine dams a small pond (Little Tipsoo Lake); outwash from the McNeeley glacier would have fed into Little Tipsoo Lake and Tipsoo Lake. Note that construction of the highway (SR 410) removed a significant portion of the moraine. LIDAR data: Mt. Rainier 2007 survey, WS DNR LIDAR Portal (2021).

The work of D.R. Crandell and U.S. Geological Survey colleagues on the glacial history of Mount Rainier, although now about 50 years old, still stands as the most comprehensive to date. Of particular relevance are a surficial geology map of Mount Rainier National Park (Crandell, 1969) and the Quaternary stratigraphy reported by Crandell and Miller (1974). Crandell's map was published at a scale of 1:48,000 and was recently digitized by the National Park Service (2018). Crandell and Miller (1974) assigned the glacier advances of the past several centuries (i.e., LIA) to the "Garda Stade". Combining their own tree-ring work with tephra mapping and the tree-ring work of Sigafoos and Hendricks (1961, 1972), they concluded that the two main periods of moraine building were 1730–1770 CE and 1830–1860 CE. Crandell and Miller (1974) also documented other episodes of moraine building in the first half of the sixteenth century and the mid-seventeenth century. However, a few Garda moraines are mantled with tephra layer W, which was thought by Mullineaux (1974) to be about 450 years old, suggesting that these moraines are older than 1500 CE (Table 1). In addition, the oldest Garda moraine of Carbon Glacier is older than trees that germinated before 1217 CE, which led Crandell and Miller (1974) to suggest that the Garda Stade began prior to 1200 CE. Such a date might not be considered by some to be part of the LIA; definitions vary but Clague et al. (2009) make a case that the LIA began about 1200 CE.

One or more pre-LIA advances on Mount Rainier are represented by moraines of similar form and extent to Garda moraines. They are overlain by tephra layer C and younger tephras, but not by tephra layer Y, and so are presumed to date between 4.4 and 2.2 ka (Table 1). Crandell and Miller (1974) attributed these moraines to the "Burroughs Mountain Stade" and estimated an age for this stade between 3.0 and 2.5 ka. We found that moraines of this age are uncommon and infer that most were overridden or obscured by subsequent LIA advances. In this paper, we informally refer to a "Burroughs Mountain advance" for these rare Neoglacial moraines.

Crandell and Miller (1974) also defined a latest-Pleistocene glacial episode, a small advance that they assigned to the "Sumas Stade" of Armstrong et al. (1965). They mapped deposits of this advance as "McNeeley Drift." Although Crandell and Miller (1974) never used the term "McNeeley advance," the label was applied by subsequent authors and we adopt it here.

https://doi.org/10.1017/qua.2023.63 Published online by Cambridge University Press

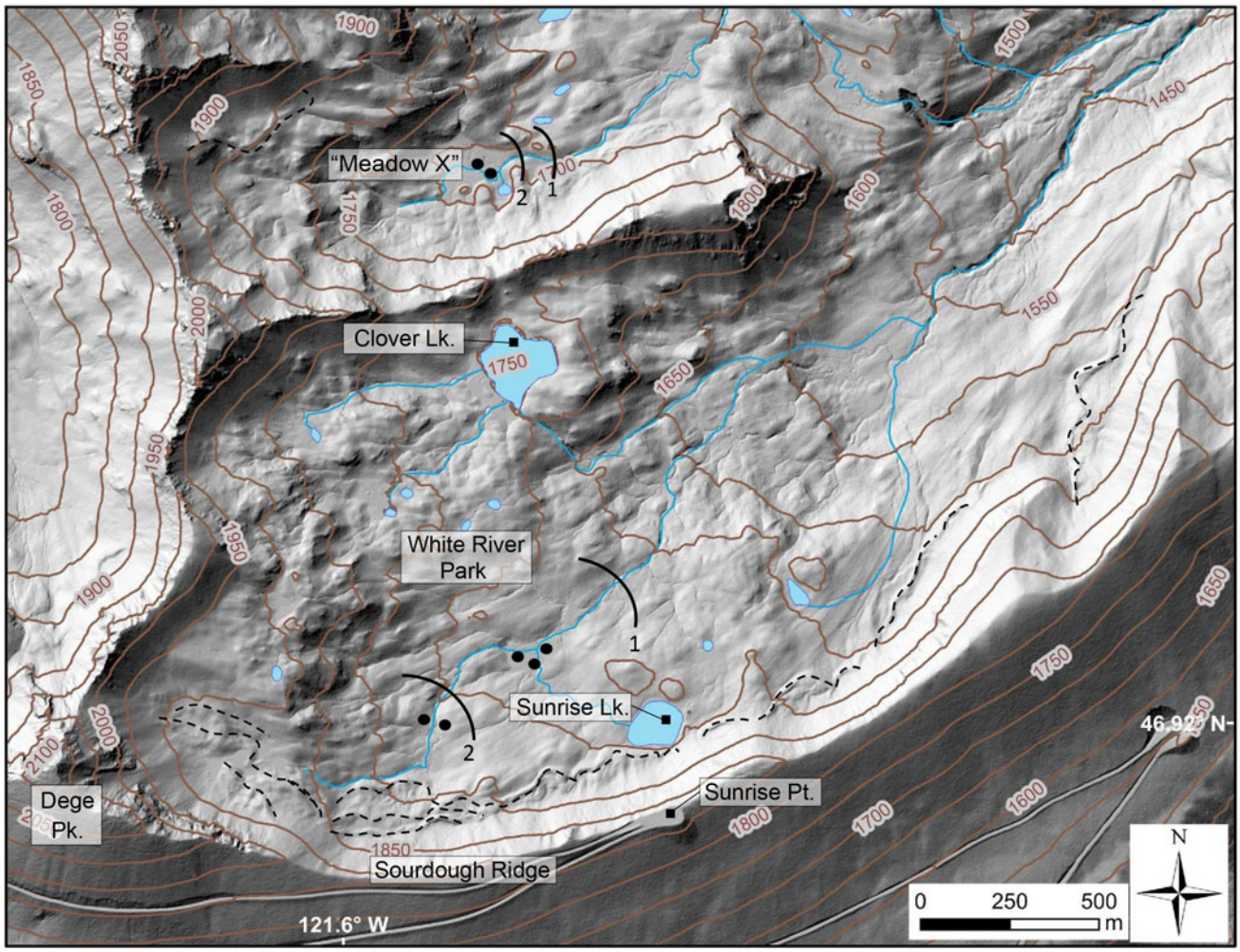

Figure 4. LIDAR image of the White River Park and Meadow X areas. Dashed lines are McNeeley moraine ridges/rock-glacier deposits. Solid black curved lines show the locations of Heine's (1998a, b) McNeeley I (downvalley) and II (upvalley) moraines. Solid black dots indicate Heine's (1998a, b) coring locations. LIDAR data: Mt. Rainier 2007 survey, WS DNR LIDAR Portal (2021).

McNeeley Drift consists of moraines overlain by R tephra (Table 1) that at the time Crandell and Miller published their report was thought to be >8.75 ka (Crandell et al., 1962). More recently, Samolczyk et al. (2016) assigned an age of about 10 ka to R tephra (Table 1); the age is discussed further and updated in this paper. McNeeley moraines are rare but where present, they typically lie up to a few hundred meters downvalley from Garda moraines. Many McNeeley deposits are moraines or relict rock glaciers within cirques or at cliff bases that show no evidence of LIA (Garda) activity; an example is the type McNeeley deposit 0.7 km south of McNeeley Peak (Fig. 2). This deposit, which appears to be, at least in part, a rock glacier complex, is discussed later in this paper. Crandell and Miller (1974) suggested that the lack of McNeeley moraines in some of the glacial valleys may indicate that McNeeley moraines were less extensive than, and likely overrun by, subsequent Neoglacial advances in these locations. They considered McNeeley deposits to be a product of a late phase of the Fraser (Late Wisconsinan) Glaciation.

Burbank (1981) dated LIA moraines on Mount Rainier using lichenometry, claiming it to be more reliable than dendrochronology. A linear extrapolation of a *Rhizocarpon geographicum* growth curve developed at Mount Rainier by Porter (1981) was considered "probably valid for 400 to 500 yr" (Burbank, 1981, p. 372), even though the oldest control point was only 140 years. Tree-ring counts were determined by Burbank (1981, p. 373) "to provide minimum ages for forested moraines where lichen growth was inhibited." Finally, Burbank (1981) concluded that the presence of a tephra on a moraine provides a reliable minimum age for moraine construction, but the absence of a tephra that is known to be in the area may not provide a reliable maximum age. He concluded that Carbon, Winthrop, North Mowich, Cowlitz, and Ohanapecosh glaciers built moraines, respectively, in the early and middle sixteenth century; early, middle, and late seventeenth century; early, middle, and late eighteenth century; early, middle and late nineteenth century; and early twentieth century. Burbank (1981) found tephra layer C (2.2 ka; Table 1) 8 m below the crest of a lateral moraine of Carbon Glacier dated using dendrochronology to older than 1217 CE by Crandell and Miller (1974; Table 1). As a result, Burbank suggested that the till of most of the east lateral moraine of Carbon Glacier predates 2.2 ka and is probably an early Neoglacial deposit of Burroughs Mountain age.

https://doi.org/10.1017/qua.2023.63 Published online by Cambridge University Press

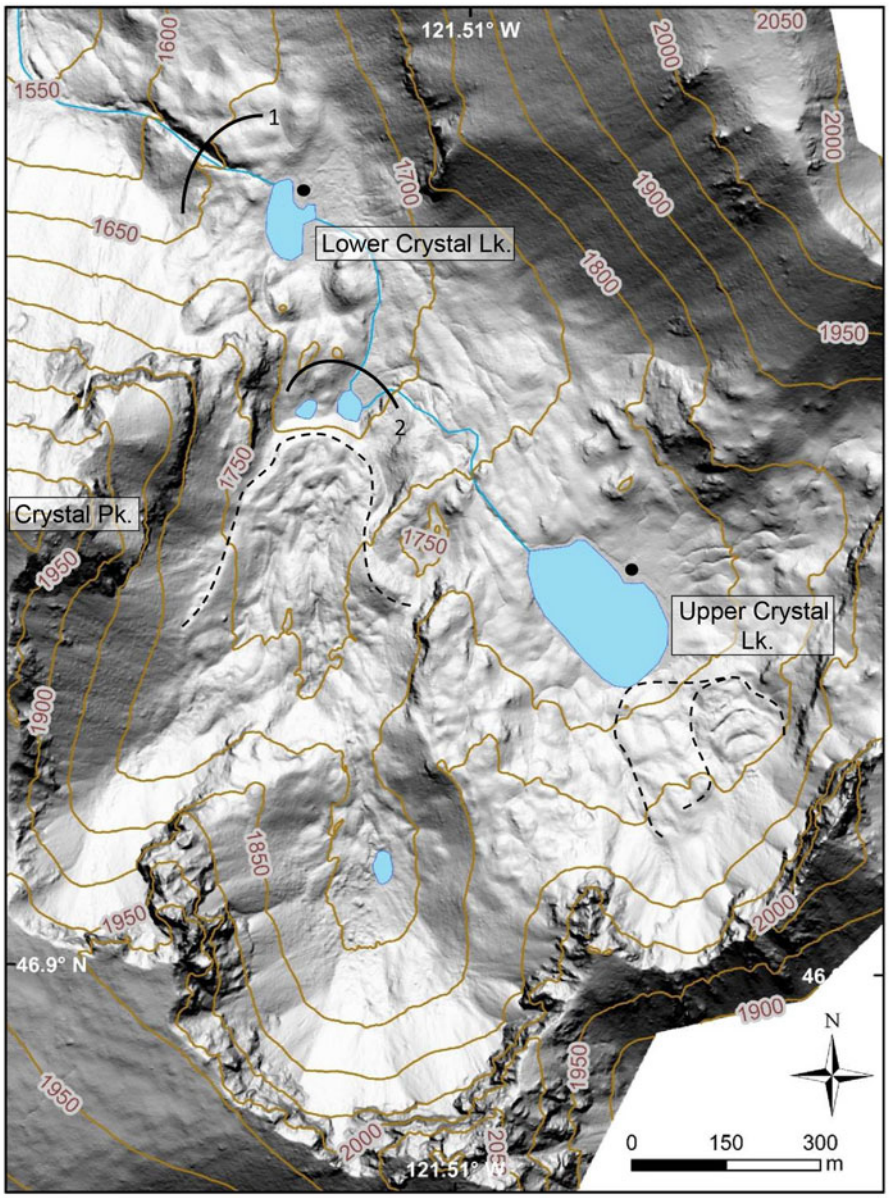

Figure 5. LIDAR image of the Crystal Lakes area. Dashed lines are McNeeley moraine ridges/rock-glacier deposits as inferred in this study. Solid black curved lines show the locations of Heine's (1998a, b) McNeeley II moraine, between upper and lower Crystal Lakes, and McNeeley I moraine, downvalley of Lower Crystal Lake. Solid black dots indicate Heine's (1998a, b) coring locations. LIDAR data: Mt. Rainier 2007 survey, WS DNR LIDAR Portal (2021).

Heine (1997, 1998a, b) remapped McNeeley moraines in an area on the northeast flank of Mount Rainier that overlapped the study area of Crandell (1969) and Crandell and Miller (1974). He also radiocarbon-dated lake and bog sediments interpreted to be associated with the moraines. Heine (1998a) mapped two moraines in several cirques and concluded that there were two distinct late-glacial advances, which he named McNeeley I and II. There is only one site in Heine's and Crandell and Miller's overlapping study areas where McNeeley moraines were mapped at the same place. That site is just above Tipsoo Lake, where Heine and Crandell and Miller recorded a single moraine (Fig. 3). At Huckleberry Park, Crandell and Miller (1974) and Heine (1997, 1998a, b) mapped a single McNeeley moraine, but in different locations with different orientations (Fig. 2). Crandell and Miller (1974) mapped no moraines at eight other sites where Heine (1998a, b) mapped double moraines.

Heine (1998a, b) reported a minimum age of ca. 13.2 ka (11.3 ^{14}C ka) for his earlier McNeeley I advance based on dates from cores taken from bogs or lakes dammed by the moraines at three sites—Upper Dewey Lake, Upper Henskin Lake, and White River Park (Fig. 1). Heine concluded that these minimum ages were close to actual ages and thus inferred that glaciers retreated from McNeeley I moraines shortly before ca. 13.2 ka, which led him to assign a pre-Younger Dryas age for his McNeeley I advance. Heine's (1997, 1998a, b) McNeeley II moraines occur adjacent to, but slightly up-valley of, McNeeley I moraines, and thus were assumed to be younger. He inferred the moraines to be older than 8.75 ka based on (1) a local cover of R tephra, then thought to be that age (Crandell et al., 1962); and (2) a minimum age of 10.28–9.99 ka (9.14 ± 0.1 ^{14}C ka) from a sediment core collected from upper Dewey Lake (Heine, 1998a, b). Heine further proposed that the McNeeley II advance occurred between 10.9 and 9.95 ka (9.80–8.95 ^{14}C ka) based on his interpretation that a layer with a lower content of organic matter than layers above and below it in cores from White River Park and Tipsoo Lake represents glaciogenic sediments from the McNeeley II advance upstream of the coring sites. Based on this assumed age range, Heine (1997, 1998a, b)

https://doi.org/10.1017/qua.2023.63 Published online by Cambridge University Press

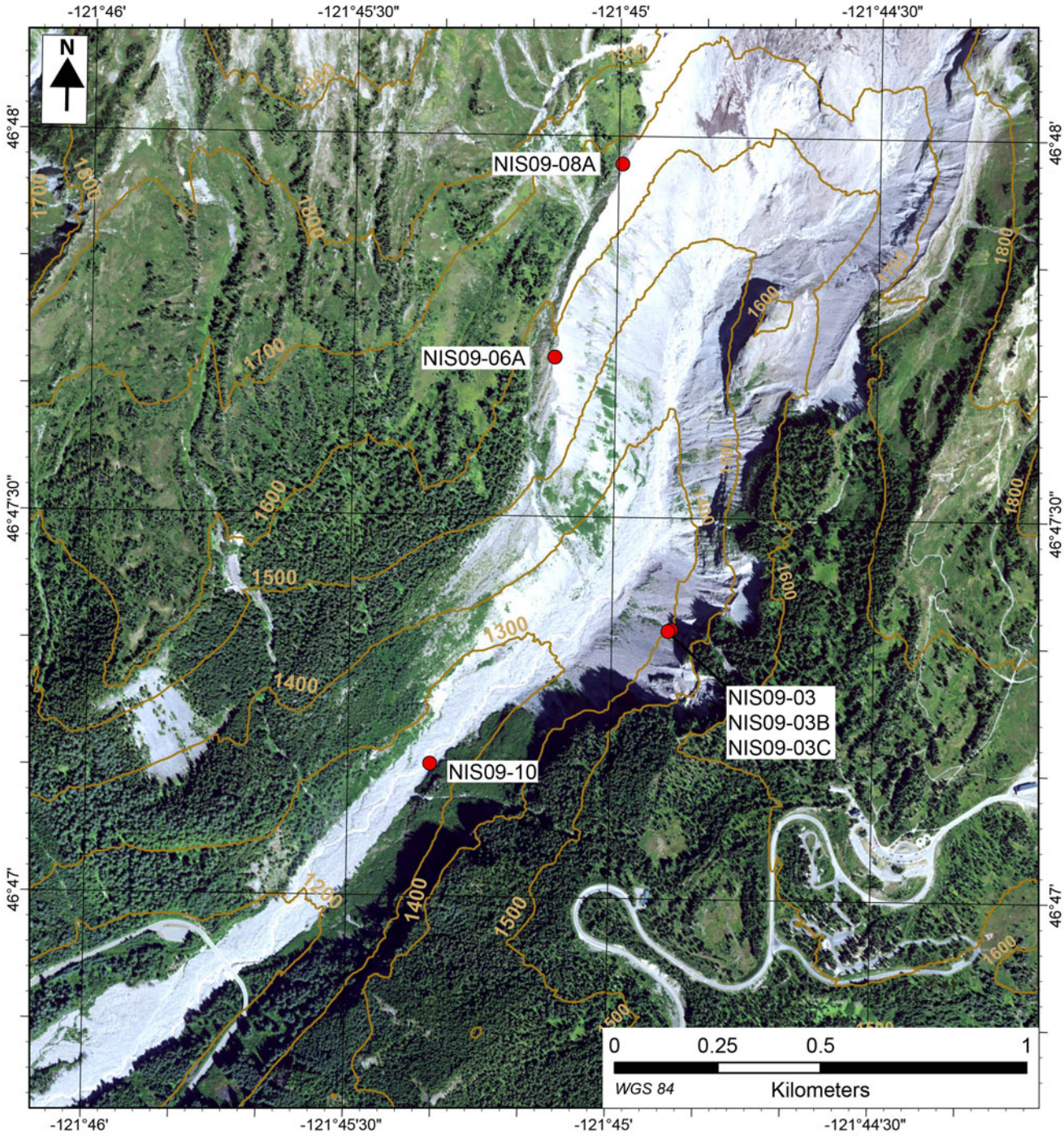

Figure 6. Aerial imagery of Nisqually Glacier and forefield showing locations of dated wood samples collected from the east and west composite lateral moraines (see also Fig. 10). Imagery data: statewide NAIP 2015 True Color (NAIP: https://registry.opendata.aws/naip) [accessed May 2023].

concluded that the McNeeley II advance post-dates the Younger Dryas event and, further, that there is no evidence of an advance during the Younger Dryas on Mount Rainier.

METHODS

Identification and mapping of pre-Neoglacial moraines

We used publicly available LIDAR data and high-resolution optical imagery available in Google Earth to identify and map moraines within the study area (Fig. 1; Supplementary Fig. 1). Bare earth LIDAR DEMs (2007–2008 survey) with a ground-sampling resolution of 1 m were downloaded from the Washington LIDAR Portal (lidarportal.dnr.wa.gov). These data were imported into ArcGIS to create hill-shade and slope-shade maps of the field area for detailed analysis. We used the LIDAR imagery to map prominent lateral and terminal latest-Pleistocene and Holocene moraines and associated periglacial deposits (e.g., protalus ramparts), evaluating the published mapping of Crandell (1969), Crandell and Miller (1974), and Heine (1998a, b).

https://doi.org/10.1017/qua.2023.63 Published online by Cambridge University Press

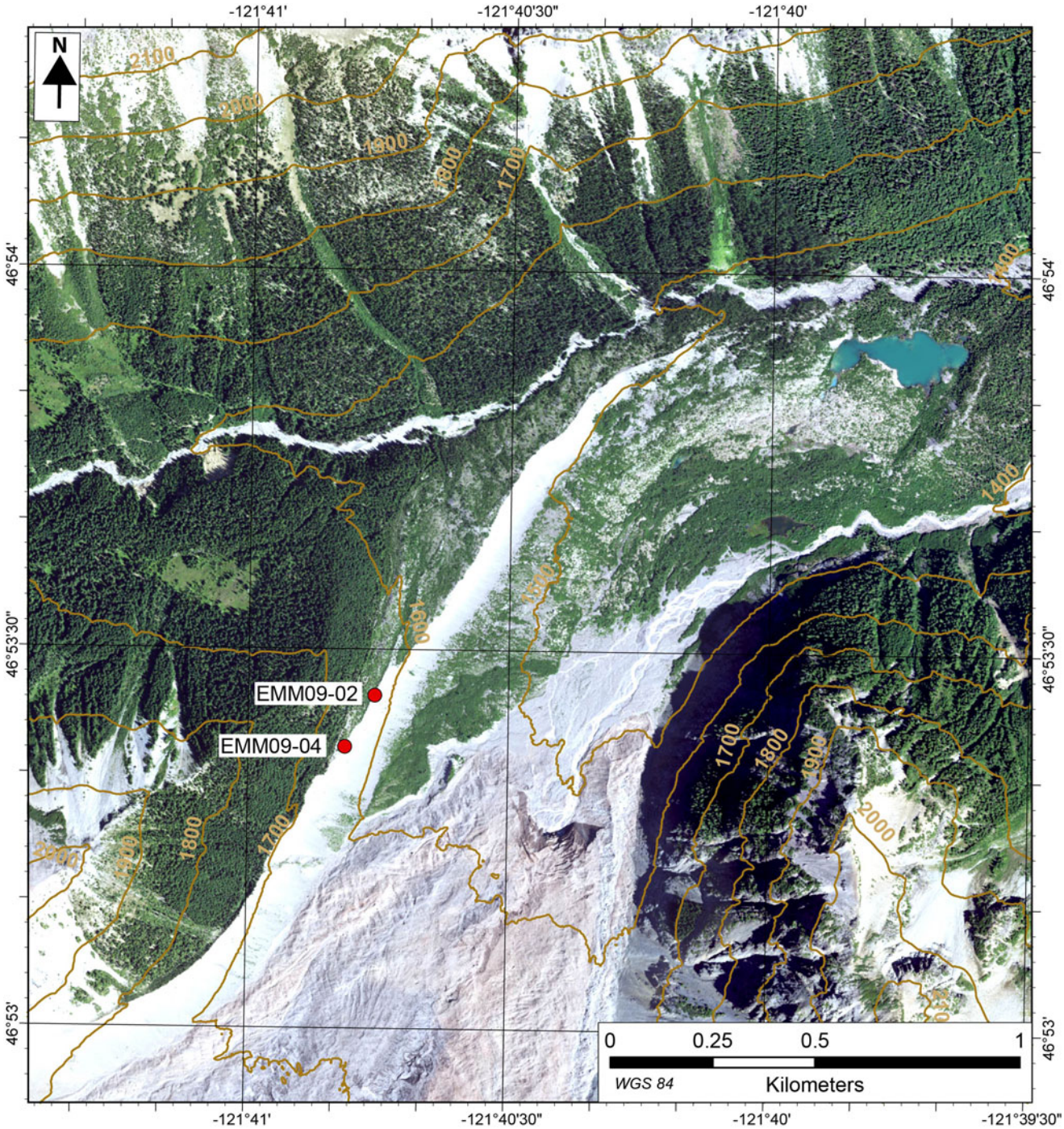

Figure 7. Aerial imagery of Emmons Glacier and forefield showing locations of dated wood collected from a west composite lateral moraine. Imagery data: statewide NAIP 2015 True Color (NAIP: https://registry.opendata.aws/naip) [accessed May 2023].

In September 2021, we visited several sites of mapped McNeeley moraines to make observations and compare them to the available imagery. To compare our LIDAR and field-based mapping to that of Heine (1997, 1998a, b) we geocoded the study map from his 1998b publication (Heine, 1998b, fig. 1) using ground control points (GCPs) obtained from hill-shade LIDAR images. Using a Helmert transformation with cubic resampling, we calculated the RMS error of the 14 GCPs to be 3.09 pixels, or about ±15 m. The original map was resampled to 5 m and projected into UTM Zone 10 N (WGS84). We also compared our results to the georeferenced digitized surficial mapping of Crandell (1969) and Crandell and Miller (1974), both of which are available through the U.S. Geological Survey's National Geologic Map Database (U.S. Geological Survey, 2023), and draped the geolocated maps in Google Earth to aid in our assessment of the previous mapping.

Lake sediment coring

We collected a sediment core from Tipsoo Lake (Figs. 1 and 3) in 2010 to provide a continuous record of sedimentation from the surrounding catchment during terminal Pleistocene and Early

https://doi.org/10.1017/qua.2023.63 Published online by Cambridge University Press

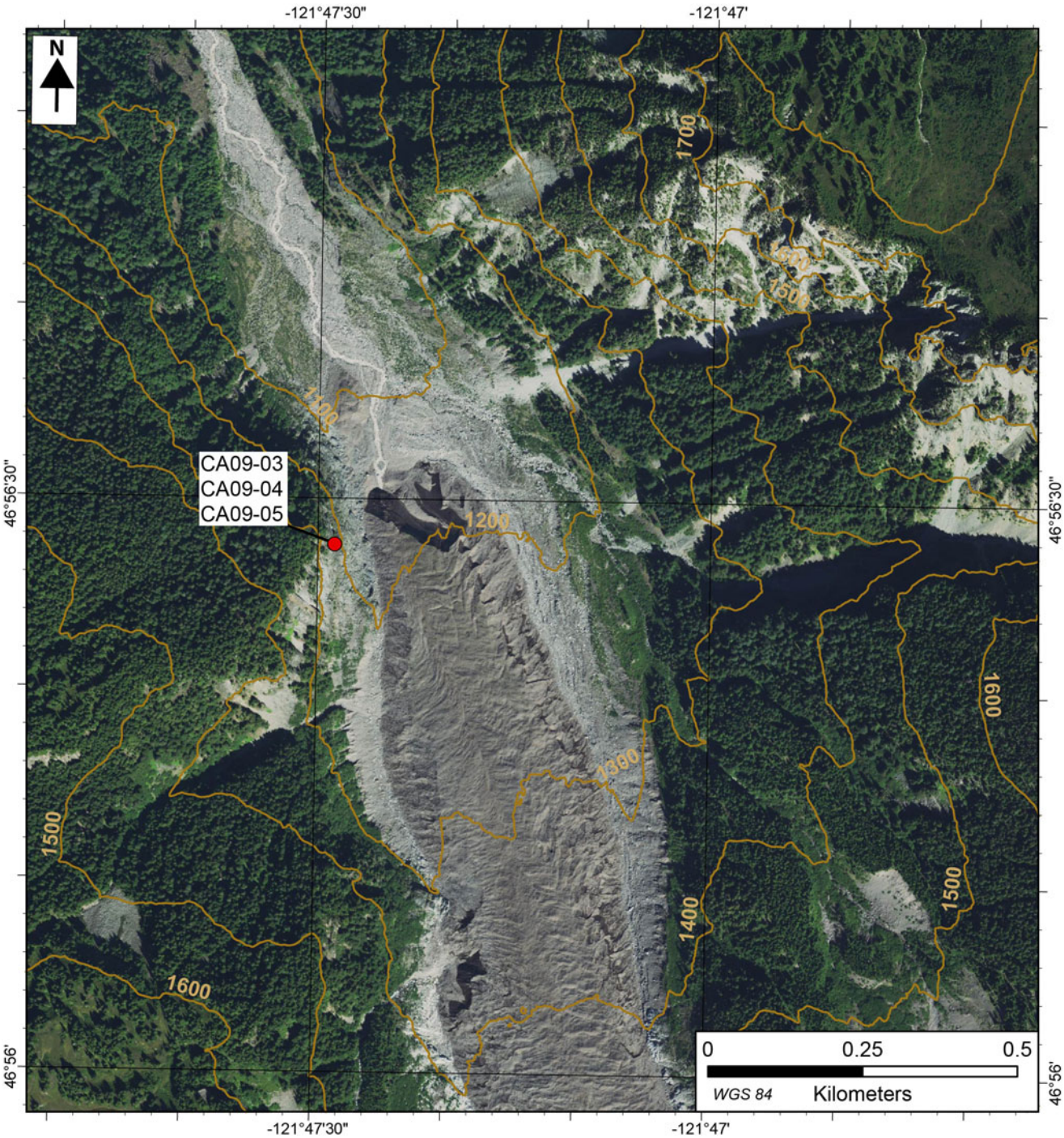

Figure 8. Aerial imagery of Carbon Glacier and forefield showing the location of dated wood samples collected from the west composite lateral moraine. Imagery data: USA NAIP imagery: natural color (https://registry.opendata.aws/naip) [accessed May 2023].

Holocene time (Karlén, 1976, 1981). We used a modified Livingstone piston-coring device operated from a floating plywood platform following the techniques of Livingstone (1955) and Wright (1967). Tipsoo Lake is located ~19 km east of Mount Rainier's summit at an elevation of ~1480 m asl. The lake basin is downstream of an ice-free, west-northwest facing cirque with a floor that lies between 1700 and 1830 m asl (Heine, 1997, 1998a, b). Bathymetric data show that the lake has a maximum depth of approximately 2.5 m. A shallow pond named Little Tipsoo Lake is located just upstream of the south end of Tipsoo Lake and is dammed by a sediment ridge identified as a McNeeley moraine by Crandell (1969) and later interpreted to be an Early Holocene McNeeley II moraine by Heine (1997, 1998a, b) (Fig. 3). There is no evidence of Neoglacial glacier activity in the cirque above Tipsoo Lake.

Sediment core sections (total length 118 cm) were analyzed at the Lake Coring Lab in the Geology Department, Western Washington University. Cores initially were scanned for magnetic susceptibility (MS) at 2-cm intervals using the Bartington MS2C Core Logging Sensor. The core sections were then split in half,

https://doi.org/10.1017/qua.2023.63 Published online by Cambridge University Press

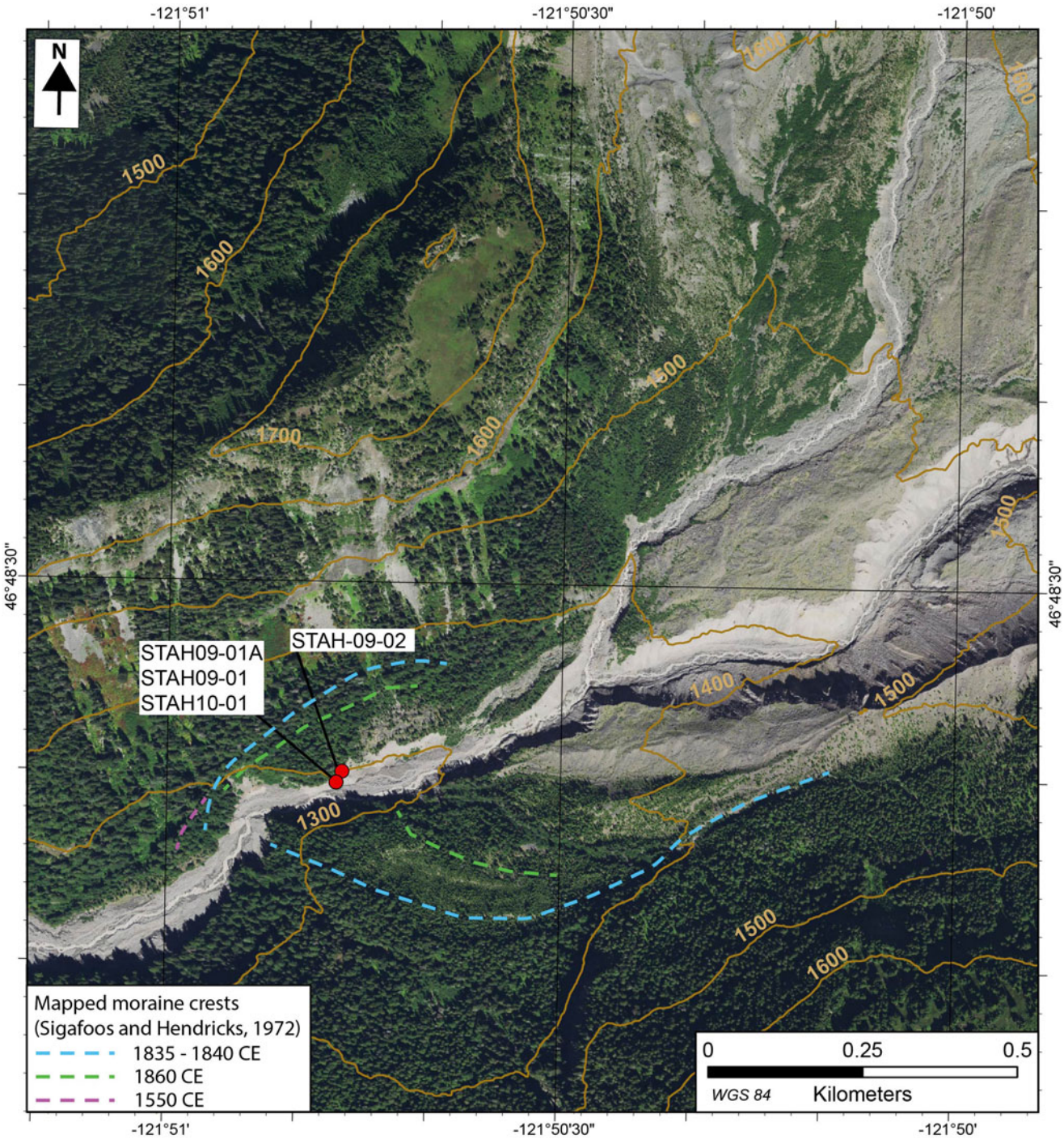

Figure 9. Aerial imagery of South Tahoma Glacier forefield and Tahoma Creek channel showing the locations of collected wood samples (see also Fig. 10). The wood was exposed in a gully eroded by Tahoma Creek. The dashed lines indicate the mapped 1550, 1835–1840, and 1860 CE lateral-moraine crests (Sigafoos and Hendricks, 1972). Imagery data: USA NAIP imagery: natural color (https://registry.opendata.aws/naip) [accessed May 2023].

photographed, and described for visual stratigraphy. We conducted detailed analyses only on the deepest section of core, from 66 to 118 cm below the lake floor, because it had the greatest potential to contain a sedimentation record from the latest Pleistocene, Early Holocene, or both. For this section, we collected samples to analyze organic matter content and the grain size of the sediments. Organic matter (OM) content was assessed using loss-on-ignition (LOI) methods adapted from Cambardella et al. (2001) and Heiri et al. (2001). We collected samples at 1-cm increments, dried them at 100°C for 14–24 hours, and then placed them in a muffle furnace at 450°C for 4 hours. Grain size was measured by laser diffraction using a Malvern Mastersizer 2000 with autosampler. Prior to grain-size analysis, we treated each sample with hydrogen peroxide (H_2O_2; 30% solution) to remove organic sediment, and with sodium hydroxide (NaOH) to remove biogenic silica. Macrofossil and bulk organic samples were

https://doi.org/10.1017/qua.2023.63 Published online by Cambridge University Press

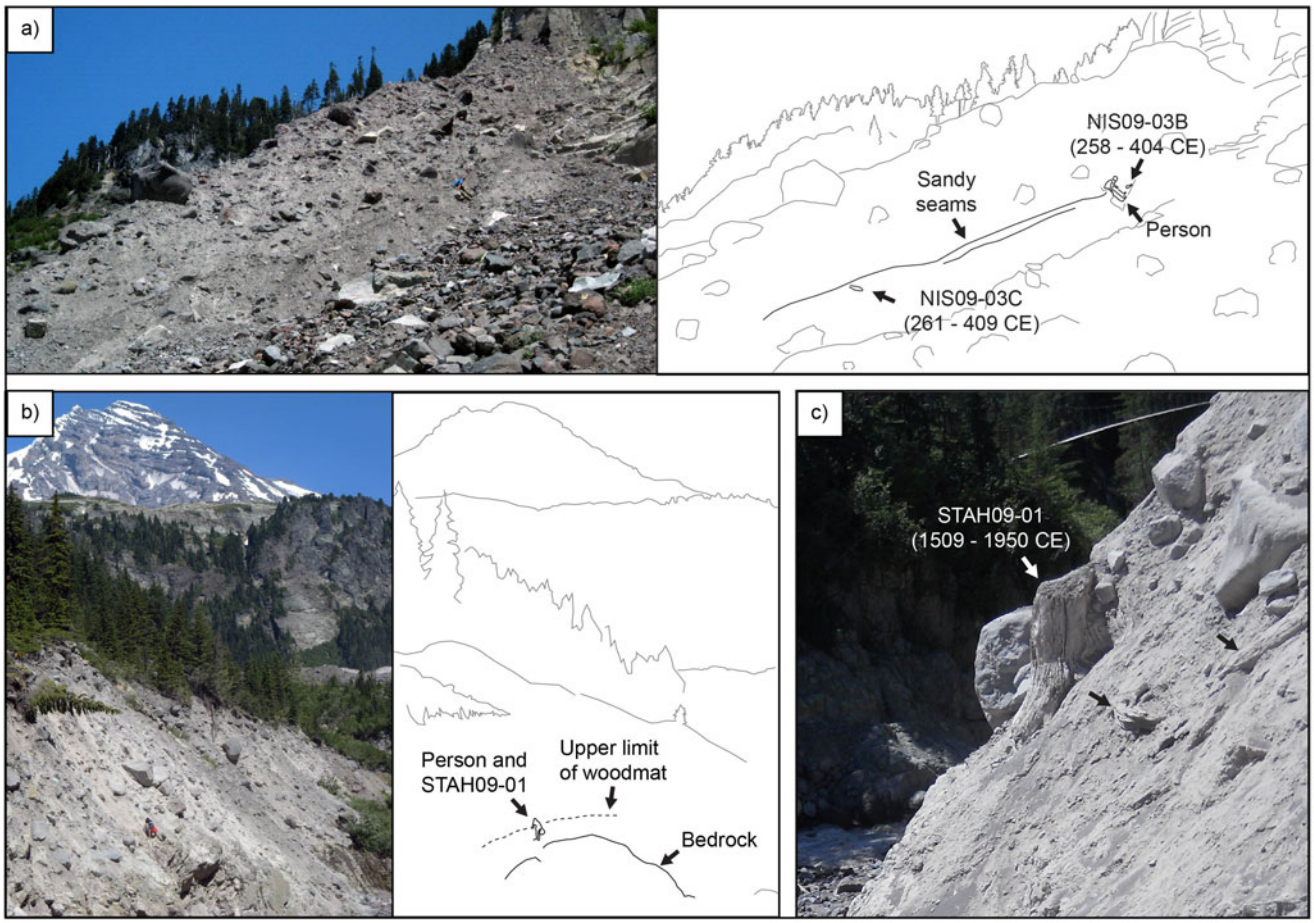

Figure 10. Images showing example stratigraphy at sample sites. (a) Image and line drawing show a gully incised into the proximal face of the east lateral-moraine crest of Nisqually Glacier (see also Fig. 6). Locations of the sandy seams along the paleosurface as well as radiocarbon-dated wood are shown in line drawing. Person for scale. (b) Image and line drawing show sediments exposed by incision on the north bank of Tahoma Creek in the forefield of South Tahoma Glacier (see also Fig. 9). Location of bedrock knob is outlined by a solid black line, and the dashed line indicates approximate upper elevation of the wood mat. Person for scale. (c) Image looking downstream. White arrow indicates the location of a large sheared stump (STAH09-01; 81 cm in diameter). Black arrows point to other wood fragments in the wood mat. Photographs by M. Samolczyk and K. Adams.

radiocarbon-dated to provide age control within the section (Table 2). Finally, we identified key tephra layers in the core based on their stratigraphic position and macroscopic characteristics. R tephra and Layer O samples were identified in the core and characterized using petrographic and geochemical techniques, as reported in Samolczyk (2011) and Samolczyk et al. (2016).

Lateral-moraine stratigraphy

Lateral moraines in many cases are composite landforms built by proximal-flank accretion or distal-flank accretion, and they consist of stacked or plastered tills of different ages deposited by multiple glacier advances (e.g., Humlum, 1978; Osborn, 1978; Röthlisberger and Schneebeli, 1979; Matthews and Petch, 1982; Small, 1983; Osborn, 1986; Ryder and Thomson, 1986; Iturrizaga, 2008; Osborn et al., 2012). Unconformities between stacked/plastered tills may be marked by paleosurfaces containing non-glacial deposits or soils, representing periods when ice was not present. Organic matter and tephra associated with paleosurfaces can be dated to provide minimum and maximum ages for underlying and overlying tills, respectively. Detrital wood fragments not associated with a paleosurface and found lodged in lateral moraines provide maximum-limiting ages of encasing tills (Röthlisberger and Schneebeli, 1979; Ryder and Thomson, 1986; Osborn and Karlstrom, 1989; Osborn et al., 2001).

The proximal flanks of the lateral moraines of Nisqually, Carbon, South Tahoma, and Emmons glaciers (Fig. 1) were inspected in the field for till packages demarcated by paleosurfaces. Samples of organic material associated with these surfaces, such as branches, roots, and stems of woody plants were collected for radiocarbon dating. To avoid inadvertently collecting modern wood, we only chose samples where the stratigraphic and exposure conditions precluded modern sources of wood and mass-wasting deposits. Wood samples were collected only if rooted (in situ) in a paleosurface buried by overlying tills, or well-lodged into till. Samples were air-dried, and the outermost rings were collected and sent for radiocarbon analysis.

Lahars and other debris flows occur frequently on the flanks of Mount Rainier, and their deposits are common in the low-lying glacial valleys surrounding the volcano (Crandell, 1971; Scott et al., 1995; Walder and Driedger, 1995; Vallance et al., 2003). Lahar deposits emplaced onto lateral moraines can be incorrectly interpreted as till. Lahar deposits at Mount Rainier are typically massive or crudely stratified, poorly sorted, and may be graded

https://doi.org/10.1017/qua.2023.63 Published online by Cambridge University Press

Table 2. Sample site locations and reported radiocarbon ages from wood in lateral moraines and glacier forefields, and macrofossil and bulk organics in lacustrine sediments in Mount Rainier National Park.

Sample identification	Latitude/Longitude (decimal degrees)	Lab ID	Lab[1]	Lateral moraine	^{14}C yr BP	Calibrated age (2σ range; median age in brackets)[2]	Sample dimension in centimeters (length × width)	Sample description[3]
Nisqually Glacier								
NIS09-03	46.78922/−121.74812	262523	Beta	east	1670 ± 50	252–538 CE (395 CE)	60 × 25	Detrital branch or stem with no bark. Angled parallel to the proximal moraine flank along sand beds.
NIS09-03C	46.78922/−121.74812	68597	Keck	east	1700 ± 15	261–409 CE (335 CE)	101 × 20	Detrital branch or stem with no bark. Angled parallel to the proximal moraine flank along sand beds.
NIS09-03B	46.78919/−121.74821	68598	Keck	east	1715 ± 15	258–404 CE (331 CE)	60 × 20	Detrital branch or stem with no bark. Angled parallel to the proximal moraine flank along sand beds.
NIS09-06A	46.79515/−121.75194	262532	Beta	west	480 ± 70	1310–1630 CE (1470 CE)	30 × 3	Detrital branch lodged into till with no bark.
NIS09-08A	46.79939/−121.74988	72647	Keck	west	595 ± 15	1308–1402 CE (1355 CE)	10 × 2	Detrital branch lodged into till with no bark.
NIS09-10	46.78623/−121.75572	68599	Keck	east	370 ± 15	1457–1622 CE (1539.5 CE)	92 × 20	In-situ stump protruding vertically from till, top 1/3 bent. No bark visible.
Emmons Glacier								
EMM09-04	46.88952/−121.68023	72648	Keck	west	345 ± 15	1478–1633 CE (1555.5 CE)	61 × 5	Detrital branch lodged into till.
EMM09-02	46.89062/ -121.68265	264797	Beta	west	270 ± 50	1476–1950 CE (1713 CE)	18 × 4	Detrital branch lodged into till.
South Tahoma Glacier								
STAH09-02	46.80558/−121.84630	72649	Keck	forefield	185 ± 15	1663–1950 CE (1806.5 CE)	120 × 38	Detrital branch or stem lodged into till.
STAH09-01A	46.80542/−121.84642	72646	Keck	forefield	140 ± 15	1673–1942 CE (1807.5 CE)	91 × 31	Detrital branch or stem appears twisted around bedrock.
STAH09-01	46.80542/−121.84642	264798	Beta	forefield	250 ± 40	1509–1950 CE (1729.5 CE)	100 × 81	In-situ sheared, splintered stump. Till is imbedded into top sheared surface.
STAH10-01	46.80542/−121.84642	90381	Keck	forefield	130 ± 20	1682–1939 CE (1810.5 CE)	65 × 35	In-situ sheared, splintered stump with roots also partly exposed. Some bark remains.
Carbon Glacier								
CA09-04	46.941/−121.79131	72650	Keck	west	1755 ± 15	243–349 CE (296 CE)	100+ × 30	Detrital branch or stem lodged into till.
CA09-03	46.941/−121.79131	83755	Keck	west	1665 ± 25	261–529 CE (395 CE)	200+ × 70	Detrital branch or stem lodged into till.
CA09-05	46.941/−121.79131	264796	Beta	west	1780 ± 40	205–404 CE (304.5 CE)	200+ × 60	Detrital branch or stem lodged into till.
Tipsoo Lake								
Tip-88	46.86964/−121.51705	90380	Keck	N/A	8905 ± 20	10.177–9.909 ka (10.043 ka)	N/A	Pine needle
Bulk 88	46.86964/−121.51705	113324	AA	N/A	9492 ± 34	11.069–10.588 ka (10.828 ka)	N/A	Bulk sample
Bulk 98	46.86964/−121.51705	113325	AA	N/A	10472 ± 35	12.620–12.191 ka (12.405 ka)	N/A	Bulk sample

1.AA = University of Arizona Accelerator Mass Spectrometry Lab; Keck = University of California Irvine W.M. Keck Carbon Cycle AMS facility; Beta = Beta Analytic Inc.; USGS = U.S. Geological Survey
2.Calibrations completed using Calib 8.2 (Stuiver et al., 2021) and the IntCal20 Northern Hemisphere radiocarbon age calibration curve (Reimer et al., 2020). Calibrated ages with a standard error >50 are rounded to the nearest decade; 2σ age ranges reported.
3.The outermost rings of each sample were collected when possible.

(Scott et al., 1995; Vallance, 2000). Deposits range in thickness from tens of centimeters to tens of meters, with thick deposits commonly occurring in valley bottoms and thinner veneers draping steep valley walls. Lahar deposits on Cascade volcanoes, unlike till, typically contain matrix vesicles, casts of wood fragments, or wood fragments themselves, and tend to be less heterolithologic than till; primary clasts are typically subangular to angular (Vallance, 2000). All sample sites in this study are in glacial valleys located in lahar inundation zones (Vallance et al., 2003). An attempt to distinguish between lahar and till deposits was made at each site, and any diamict having lahar characteristics was not considered a part of the glacier fluctuation record.

Radiocarbon age calibration and conventions

Samples were dated using radiocarbon methods at Beta Analytic Inc. (Miami, USA), the Accelerator Mass Spectrometry Lab at the University of Arizona (Tucson, USA), and at the W.M. Keck Carbon Cycle Accelerator Mass Spectrometer facility at the University of California Irvine (Irvine, USA) (Table 2). We calibrated radiocarbon ages using the IntCal20 Northern Hemisphere radiocarbon age calibration curve of Reimer et al. (2020) in Calib 8.2 (Stuiver et al., 2021). Calibrated radiocarbon ages are reported as 2σ ranges and rounded to the nearest half decade if the reported error is larger than 50 years. Radiocarbon ages are presented as calendar ages (CE) when younger than 1 CE; older calibrated radiocarbon ages are presented as thousand years before present (ka), where "present" is considered to be 1950 CE.

RESULTS

Moraine record

Based on our mapping, two distinct groups of moraines exist in the study area. A third group, described by Crandell and Miller (1974), is less definitive. The first group comprises sparsely vegetated, often sharp-crested, and poorly consolidated deposits close to contemporary glaciers. In most cases, the first group denotes glaciers that were 0.5–1.5 km more extensive than present-day glaciers (as of 2022). These features are products of the Little Ice Age or Garda Stade of Crandell and Miller (1974), are hereafter referred to as 'late Neoglacial moraines', and are equivalent to those recognized in previous work (Sigafoos and Hendricks, 1972; Burbank, 1981).

The second distinct group of moraines, hereafter referred to as 'McNeeley moraines', as per Crandell and Miller (1974), or more generally 'pre-Neoglacial moraines', are stable vegetated landforms that either occupy cirque basins in which no glaciers exist today or lie up to a few hundred meters beyond Neoglacial moraines. These landforms include classic cirque moraines as well as deposits that could be protalus ramparts or small rock glaciers (Crandell and Miller, 1974). Examples of these features include the McNeeley type deposit (Fig. 2) and the end moraine just upstream from Tipsoo Lake (Fig. 3). Some of these landforms have multiple crests.

The third, less-definitive moraine group comprises the 'Burroughs Mountain moraines' of Crandell and Miller (1974), who provided four examples. The moraines are described as being older than Garda moraines because they are overlain by 2.2 ka tephra C, but younger than McNeeley moraines because they seem not covered by 4.4–3.6 ka tephra Y (Table 1). However, this interpretation is somewhat ambiguous because the absence of a tephra does not provide a definitive maximum age, and a moraine can be younger than an overlying tephra if the tephra has been reworked. Both points were acknowledged by Crandell and Miller (1974).

Pre-Neoglacial moraines

Our mapping of McNeeley moraine crests using LIDAR data largely accords with the locations of McNeeley deposits identified by Crandell (1969; Figs. 2 and 3). The much higher resolution of the bare-earth LIDAR data, however, allows a better definition of the extent and morphologies of the deposits. Also, we found more morainal deposits than Crandell (1969). Comparison of our mapping and that of Crandell differs from that reported by Heine (1997, 1998a, b). Of the 17 McNeeley moraines identified by Heine (1997, 1998a, b), our analysis corroborates only a single deposit: the Tipsoo Lake moraine (Fig. 3). In most basins where Heine mapped McNeeley moraines, we find no evidence for such deposits. In a few cirques, Crandell (1969) and our mapping show McNeeley deposits close to the headwalls, but not at locations mapped by Heine (1997, 1998a, b), which typically lie 0.5–1.0 km downvalley and 200 m lower than the deposits that we have mapped as McNeeley moraines. Below we provide a few examples of the differences in our and Heine's interpretations.

White River Park

The McNeeley moraines mapped by Heine (1997, 1998a, b) in the vicinity of Sunrise Lake (Fig. 4) are low, rounded ridges adjacent to and below the meadows cored by Heine. These ridges all have a general orientation parallel to the valley axis, rather than across it. The taller ridges typically have bedrock cores, whereas the lower ridges are generally smoother and lack boulders. Exposures in the lower ridges from creek incision reveal sandy, tephra-rich sediment with scattered subangular clasts. These deposits are unlike glacial till so, combined with their orientation, we disagree with the interpretation that the landforms are terminal moraines impounding the meadows as mapped by Heine (Fig. 4). The only deposits that we interpret to be McNeeley age are the small protalus deposits that lie at the foot of cirque headwall slopes above and south of the meadows (Fig. 4).

Meadow X

"Meadow X" lies immediately north of White River Park (Fig. 4). At this site, Heine (1997, 1998a, b) described a pronounced moraine at the northeast end of the meadow. He interpreted this moraine to be McNeeley II in age and inferred that a less-distinct McNeeley I moraine occurred a short distance downvalley. Both LIDAR and field observations reveal no moraines in the vicinity of the meadow. Heine's McNeeley II moraine is a bedrock ridge and has no till exposures or erratics on the surface. As at White River Park, LIDAR imagery shows no evidence of cross-valley terminal-moraine loops or any lateral moraines upvalley in the vicinity of the meadow cored by Heine (1997, 1998a, b). Instead, the terrain appears to be dominated by bedrock-cored ridges that are dominantly oriented parallel to the valley axis. The only deposits that might be correlative to McNeeley deposits are small boulder-rich ridges at the foot of the valley headwall (Fig. 4).

Huckleberry Park

In Huckleberry basin near the McNeeley type locality of Crandell and Miller (1974), Heine (1997, 1998a, b) mapped a McNeeley II moraine just north and immediately downstream of a meadow

https://doi.org/10.1017/qua.2023.63 Published online by Cambridge University Press

that he cored (Fig. 2). The moraine mapped by Heine is downvalley of and oblique to the prominent sinuous ridge mapped by Crandell (1969), Crandell and Miller (1974), and us (Fig. 2). Our field observations at the site support observations made from the LIDAR imagery that there are no terminal or lateral moraines downstream of Heine's coring sites. Similar to the White River Park and Meadow X sites (Fig. 4), small hills and ridges downvalley from the meadow are longitudinally aligned with the valley axis and are cored by bedrock that crops out near their ridge lines. We observed no glacial deposits in Huckleberry Park other than those of Crandell and Miller's (1974) type deposit.

Crystal Lakes

Heine (1997, 1998a, b) mapped a McNeeley I moraine just downvalley of Lower Crystal Lake and a McNeeley II moraine in front of a small pond upvalley of the lake (Fig. 5). LIDAR imagery shows no moraines at these locations. We identified two older moraines that may be of McNeeley age (1) located upvalley of Upper Crystal Lake, and (2) originating from two cirques southwest of Upper Crystal Lake, between the upper and lower lakes.

Neoglacial moraines

Fifteen radiocarbon ages from wood fragments collected from unconformities within till sequences exposed in the lateral moraines of Nisqually, Emmons, Carbon glaciers, and South Tahoma Glacier forefield (Fig. 1) constrain the ages of Neoglacial glacier advances on Mount Rainier (Table 2). These ages complement and expand the existing Neoglacial record based on tree rings, lichenometry, and tephrostratigraphy.

Nisqually Glacier

We collected wood samples from two sites on the east lateral moraine of Nisqually Glacier (Fig. 6). At site 1, located approximately 700 m upvalley from the Paradise–Longmire Road bridge, a stump (NIS09-10) in growth position protruding from till 11.6 m above the base of the moraine yielded an age of 1457–1622 CE. At site 2, ~700 m upvalley from site 1, a gully cut into the lateral moraine exposed three wood fragments approximately half-way up the proximal flank of the lateral moraine. A branch or stem (NIS09-03) protruding from the downvalley gully wall returned an age of 252–538 CE. A paleosurface, roughly 9 m below site 2 along the upvalley gully wall, is marked by wood-bearing coarse sand beds (<0.5 m thick) that extend parallel to the proximal moraine flank for approximately 20 m, indicating growth of the lateral moraine by accretion of a till sheet onto the proximal flank (proximal accretion); the sand beds separate the two till sheets. Two tree branches or stems (NIS09-03B and NIS09-03C) protruding from the sand beds along the paleosurface yielded ages of 258–404 CE and 261–409 CE.

A paleosurface in the west lateral moraine of Nisqually Glacier (Fig. 6), which ranges from 3 to 10 m below the moraine crest and is exposed over a distance of about 600 m, contained at least six protruding wood fragments lodged into tills, but not rooted. Two branches, NIS09-06A and NIS09-08A, located 10 m and 4 m below the moraine crest, respectively, returned ages of 1310–1630 CE and 1308–1402 CE.

Emmons Glacier

Multiple nested lateral moraines in the Emmons Glacier forefield are parallel to the valley axis. We collected samples at two sites on the innermost moraine crest about 500 m upvalley from where Sigafoos and Hendricks (1972) dated moraine crests using dendrochronology (Fig. 7). At site 1, five wood fragments protruded from a paleosurface ~6 m below the moraine crest. The paleosurface was traced for ~135 m in a line parallel to the crest. One branch (EMM09-02) in this collection of wood samples yielded an age of 1476–1950 CE. At site 2, located 135 m upvalley from site 1, a protruding branch (EMM09-04) ~6 m below the moraine crest returned an age of 1478–1633 CE.

Carbon Glacier

We collected and dated wood from two sites on the west lateral moraine of Carbon Glacier (Fig. 8). A gully at site 1 exposed several pieces of wood in a layer ~9 m below the moraine crest. Two wood branches or stems (CA09-03 and CA09-04) yielded ages of 261–529 CE and 243–349 CE. A gully through the moraine at site 2, 60 m upvalley from site 1 and roughly at the same elevation, exposed several pieces of wood. A wood branch or stem (CA09-05) returned an age of 205–404 CE. Several wood fragments lodged in till were found at a level 7–11 m below the moraine crest in two gullies, delineating a paleosurface extending between sites 1 and 2.

South Tahoma Glacier

We collected wood samples from two sites where Tahoma Creek has incised into till in the forefield of South Tahoma Glacier, ~150 m upvalley from the Wonderland Trail bridge (Fig. 9). The two sites are located along the near-vertical, north gully wall above Tahoma Creek, ~150 m upvalley from nested LIA terminal moraines. These terminal moraines extend upvalley into heavily vegetated lateral moraines, which were dated to ca. 1550, 1835–1840, and 1860 CE by Sigafoos and Hendricks (1972) using dendrochronological methods (Fig. 9).

At site 1, a wood mat comprising sheared stumps in growth position, roots, and branches lies 12 m below the crest of the gully wall. The wood mat is covered by till and lies on a nearly vertical bedrock surface cropping out in the gully wall above Tahoma Creek (Fig. 10). The outer rings of two large sheared stumps (STAH09-01 and STAH10-01; 81 and 35 cm in diameter) in growth position and a branch or stem (STAH09-01A) yielded ages of 1509–1950, 1682–1939, and 1673–1942 CE, respectively. At site 2, ~30 m upvalley from site 1, a stem or branch (STAH09-02) protruding from till 15 m below the crest of the gully wall returned an age of 1663–1950 CE. The large calibrated age ranges of these three samples owes to the broad 2σ confidence interval in the radiocarbon calibration curve for samples that date to around 300 ^{14}C yr BP (Niklaus et al., 1994). We exclude the possibility that the wood mat is modern and is from vegetation that grew on the gully wall since the latest glacier advance, based on the complete absence of large trees growing on the steep gully walls of Tahoma Creek in the area where dated samples were collected and the concentration of wood in a layer below the thick (12–15 m) package of diamict. Several lahars have inundated the Tahoma Creek drainage during the Holocene (Walder and Driedger, 1994). However, the diamict covering the exposed wood does not contain sedimentological features that indicate deposition by a lahar (e.g., vesicles, gradation, and laminations). In addition, the sites are located in a zone of debris conveyance rather than deposition (Walder and Driedger, 1994); thus we conclude that the thick package of diamict (~12 m thick) overlying the wood mat is till.

https://doi.org/10.1017/qua.2023.63 Published online by Cambridge University Press

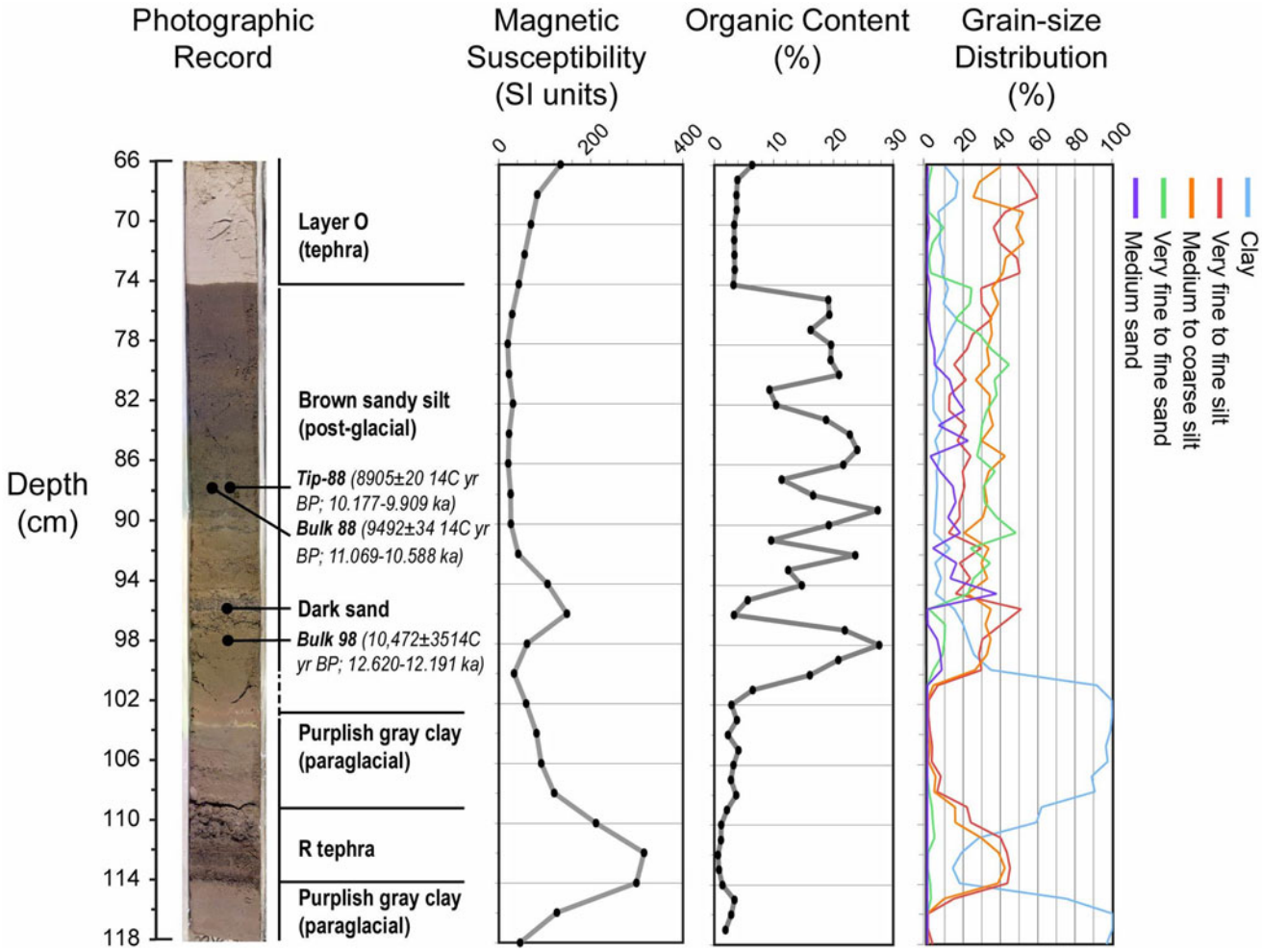

Figure 11. Stratigraphy of Tipsoo Lake core. Photograph at the left shows simplified lithostratigraphy with the location of R tephra (108.5–114 cm) and position of radiocarbon-dated samples. Magnetic susceptibility indicates peaks at about 96 cm and 112 cm; the stratigraphically lower peak corresponds to R tephra, and the upper peak corresponds to a probable unidentified tephra. Organic content is highest in the brown sandy silt unit and lowest in the clay unit. Paraglacial sediments are shown by a decrease in grain size to clay between 100 and 118 cm depth, except for where R tephra occurs.

Lacustrine record

The analyzed 52-cm-long section of the Tipsoo Lake core comprises three primary sedimentologic units, from top to bottom (Fig. 11): (1) silt-dominated tephra (layer O; 66–74 cm); (2) brown sandy silt with minor dark sand laminae (74–100 cm); and (3) purplish gray, well-sorted laminated clay (100–118 cm) containing internally bedded grayish brown tephra and lapilli (R tephra; 108.5–114 cm). Although not analyzed in detail, we note that sediments above 66 cm are visually equivalent to the brown sandy silt of unit 2 and are interlayered with tephra deposits.

Maxima in magnetic susceptibility (MS) in the Tipsoo Lake core coincide with identified tephra layers O and R (Samolczyk, 2011; Samolczyk et al., 2016) (Fig. 11). MS is relatively high in layer O (147.7 SI) and is consistently low (<30 SI) in the underlying brown sandy silt. A 1-cm-thick layer containing dark sand-sized grains at 95–96 cm depth, within the brown sandy silt, has relatively high magnetic susceptibility (147.7 SI; Fig. 11). The sand is most likely an unidentified tephra deposit rich in ferromagnetic minerals, similar to the unidentified deposits described by Mullineaux (1974) and Hobson (1976). MS rises again at 100 cm depth where the sediment first becomes clayey and is highest between 108.5–114 cm where R tephra is present, peaking at 112 cm (315.4 SI). MS drops sharply in clays underlying R tephra and reaches a value of 40 SI at the bottom of the core (118 cm depth).

Loss-on-ignition, a measure of organic-matter content, is consistently low (4%) in layer O, but abruptly increases in the brown sandy silt between 74 and 100 cm, with values ranging between about 8% to 28% (Fig. 11). The dark sand layer (95–96 cm), which is a probable tephra layer, has a low LOI value (5%). LOI decreases as the brown sandy silt grades into purplish gray clay at 100 cm, and remains consistently low to the bottom of the core at 118 cm (≤4%). LOI is lowest (<2%) in the R tephra horizon (108.5–114 cm).

Two tephra layers and three radiocarbon ages (one from a plant macrofossil and two from bulk sediment) provide age control for the Tipsoo Lake core (Table 2). Layer O, at 66–74 cm depth, is a conspicuous, exotic silicic tephra produced during the eruption of Mount Mazama at 7.777–7.477 ka (Zdanowicz et al., 1999; Egan et al., 2015; Fig. 11; Table 1). R tephra, at 108.5–114 cm depth, is easily recognizable in stratigraphic sections because it is the only lapilli-bearing tephra deposit

https://doi.org/10.1017/qua.2023.63 Published online by Cambridge University Press

underlying layer O (Crandell and Miller, 1974; Heine, 1998a; Samolczyk et al., 2016; Fig. 11). R tephra has a modeled age of 10.13–9.96 ka (Samolczyk et al., 2016), and new age constraints on R tephra, discussed later in this paper, from a sediment core taken from Tipsoo Lake suggest it could be as old as >11.6 ka. A pine needle collected at 88 cm depth, between tephra layers O and R, dates to 10.177–9.909 ka. Bulk sediment samples at 88 cm and 98 cm depth date to 11.069–10.588 ka and 12.62–12.191 ka, respectively (Table 2).

DISCUSSION

Latest Pleistocene/Early Holocene events

Moraine record

The extent, downvalley position, and groups of pre-Neoglacial moraines mapped by us broadly accord with the McNeeley deposits recognized and named by Crandell (1969) and Crandell and Miller (1974). In contrast, that mapping and our confirming re-evaluation differ from those of Heine (1997, 1998a, b) who suggested (1) two distinct McNeeley advances, and (2) substantially greater downvalley extents of McNeeley glaciers. In all but two cases, we did not confirm the moraines mapped and described by Heine (1997, 1998a, b). In some catchments (e.g., White River Park, Crystal Lakes), we identified and mapped moraines possibly of McNeeley age, but they were many hundred meters upvalley from Heine's mapped extents. Given our doubt regarding Heine's (1997, 1998a, b) mapping, we conclude that the ages he ascribed to McNeeley moraines provide little or no information regarding the glacial history of Mount Rainier. Our interpretation is that the McNeeley moraines as mapped by Crandell and Miller (1974) and in this study are consistent with a single glacier advance older than R tephra.

Lacustrine and bog sediment record

Clastic-rich intervals of proglacial lake sediment with low organic matter (OM) content are a proxy record for glacial or paraglacial conditions in a catchment in which biological productivity is low and/or minerogenic input is high (e.g., Church and Ryder, 1972; Karlén and Matthews, 1992; Leonard and Reasoner, 1999; Matthews et al., 2000; Nesje et al., 2001; Bilderback, 2004; Menounos et al., 2005; Osborn et al., 2007). Grain-size variations in proglacial lake sediments may reflect activity of warm-based glaciers, and several studies infer that organic-poor, clay- and silt-sized particles are indicators of active glaciation (e.g., Matthews et al., 2000; Nesje et al., 2001; Bakke et al., 2005; Bowerman and Clark, 2011). However, factors affecting sedimentation, such as transport distance, sediment lithology, lake size, and sediment traps, also affect the characteristics and stratigraphy of proglacial sediments (Smith, 1978; Matthews et al., 2000).

We interpret the brown sandy silt underlying layer O between 74 and 100 cm in the Tipsoo Lake core to be non-glacial in origin because of the high LOI and relatively low MS values (Fig. 11). At 100 cm depth, the organic-rich sandy silt grades into the underlying clay-rich sediments, referred to as "purplish gray clay" in Fig. 11. The clay continues to the base of the core at 118 cm, interrupted only by the R tephra at 108.5–114 cm. The clay is unique to depths 100–118 cm and is not observed elsewhere in the lacustrine sedimentation record (0–100 cm). The clay is well sorted and has a low LOI (≤4%) and higher MS values than the overlying brown sandy silt. The clay that is stratigraphically above and below R tephra has the same properties, thus we interpret that it is one unit from the same source that is interrupted by the deposition of R tephra. Because R tephra post-dates deposition of the McNeeley moraines and the clay is a single unit that pre- and post-dates the R tephra, the clay is assumed to be unrelated to glacier advance upstream. Therefore, the clay unit is likely associated with paraglacial conditions during or after the retreat phase of the McNeeley advance. Little Tipsoo Lake, located up-stream from Tipsoo Lake, may have acted as a sediment trap for any coarser grains during this period of sedimentation (Fig. 3).

Rainier R tephra at 108.5–114 cm provides an age constraint for paraglacial conditions in the cirque above Tipsoo Lake and for the McNeeley advance that built the upstream moraine (Figs. 11 and 13). The calibrated median age of 10.05 ka for Rainier R tephra reported in Samolczyk et al. (2016) was modeled from five bulk sediment or macrofossil ages from three locations on Mount Rainier (Heine, 1997, 1998a, b; Samolczyk et al., 2016). Two new bulk sediment radiocarbon ages from our Tipsoo Lake core, one from 88-cm depth with a LOI value of ∼18%, and one from 98 cm depth with a LOI value of ∼28% and sitting just above the transition to clay at 100 cm depth, calibrate to median ages of 10.83 ka and 12.41 ka, respectively (Table 2). Sometimes bulk radiocarbon ages are erroneously older than macrofossil ages from the same stratigraphic horizon (e.g., Barnekow et al., 1998; Grimm and Nelson, 2009; Wu et al., 2011). Indeed, in our Tipsoo Lake sediment core, the calibrated median bulk sediment age of 10.83 ka from 88 cm depth is about 780 years older than the calibrated median age of the macrofossil, 10.05 ka, from the same 88 cm depth. If that age offset is assumed to be about the same lower in the core, the calibrated median bulk sediment age of 12.41 ka at 98 cm depth can be corrected by subtracting 780 years, leading to an age of 11.6 ka for sediment at 98 cm depth. That would indicate R tephra is considerably older than the age of 10.05 ka previously published in Samolczyk et al. (2016).

The 98 cm depth bulk sample with the 11.6 ka age lies 10 cm above the top of R tephra in the Tipsoo Lake sediment core, with an unknown timespan of clay deposition between the two. We propose that age be considered as the new minimum-limiting age of R tephra, which suggests that the McNeeley moraines that were deposited before R tephra could have been formed during the Younger Dryas interval (Fig. 13).

Heine (1997, 1998a, b) also recovered a sediment core from Tipsoo Lake, but his interpretation of those sediments differs from our own work. Heine did not identify R tephra in his core 13, leading him to interpret that Tipsoo Lake was not within the fallout area of R tephra. Our core contains R tephra, a visually distinct, coarse, pumiceous tephra layer, between 108.5 and 114 cm depth (Fig. 11; Samolczyk et al., 2016), which suggests that the sediment record in Heine's core 13 is incomplete. An impenetrable horizon was encountered by Heine (1997, 1998a, b) at the base of his core (∼78 cm sediment depth); although the basal sediments were not observed, they were interpreted as basal till from the McNeeley I advance (Jan Heine, personal communication, 2011).

The McNeeley advance

As described above, our inspection of LIDAR and Google Earth imagery, in conjunction with ground observations failed to confirm the double McNeeley moraines mapped by Heine (1997, 1998a, b). We identified a single moraine above Tipsoo Lake, as did Heine (Fig. 3). Similarly, we agree that there is a well-defined McNeeley deposit near where Heine mapped a McNeeley II

https://doi.org/10.1017/qua.2023.63 Published online by Cambridge University Press

moraine in the Crystal Lakes basin, but his lower 'McNeeley I' moraine appears to be bedrock-cored hummocks, not a discrete terminal moraine (Fig. 5). We also found that Heine's McNeeley II moraine is mislocated: Heine mapped his moraine downvalley of a small pond in the drainage; LIDAR imagery demonstrates that the probable McNeeley deposit is immediately upvalley of the pond. The closest landform to a two-moraine McNeeley-age deposit in the study area may be Crandell and Miller's (1974) type McNeeley deposit, which extends northward from Sourdough Ridge, southeast of McNeeley Peak (Fig. 2). This deposit is sourced from two adjacent cirques and is at least partly a relict rock glacier complex. The western part of the feature is stepped and conceivably could represent a minor re-advance after a first advance, but the eastern part has just one front. In any case, many rock glaciers have superposed lobes (e.g., Dusik et al., 2014) that may be dynamic rather than climatic in origin (e.g., Loewenherz et al., 1989). Crandell (1969) and Crandell and Miller (1974) regarded the type McNeeley deposit to represent a single advance, and we see no compelling evidence to conclude otherwise.

The absence of sets of paired late-glacial cirque moraines in the area, combined with an interpretation of the lacustrine record from Tipsoo Lake, support Crandell and Miller's (1974) original notion of a single McNeeley advance on Mount Rainier. The only age constraint on the advance remains the minimum age provided by R tephra, which we propose is >11.6 ka.

Cirque glacier expansion at Younger Dryas time in western Canada (Menounos et al., 2017) and at Mount Baker (Osborn et al., 2012), which is close to Mount Rainier, suggests that the most parsimonious interpretation is a Younger Dryas timing for the McNeeley moraines (Fig. 13). However, we cannot be certain with the data at hand.

Early Neoglacial events

Given the sparse geomorphic evidence and dating challenges, we regard the ca. 4.4–2.2 ka Burroughs Mountain advance at Mount Rainier to be a tentative event (Fig. 13). Some of Crandell and Miller's (1974) Burroughs Mountain moraines could be McNeeley or Garda in age, as they acknowledged. An early Neoglacial, LIA-scale advance of glaciers between about 3 and 2 ka would not be unexpected, since the Tiedemann and Peyto advances of similar age have been documented in the Coast and Rocky Mountains of western Canada (e.g., Ryder and Thompson, 1986; Luckman et al., 1993; Menounos et al., 2009), but evidence of such an advance on Mount Rainier remains scant.

Later Neoglacial events

Dendrochronologic and lichenometric dates of end and lateral moraines from Sigafoos and Hendricks (1972) and Burbank (1981) provide minimum ages of moraine surface stabilization,

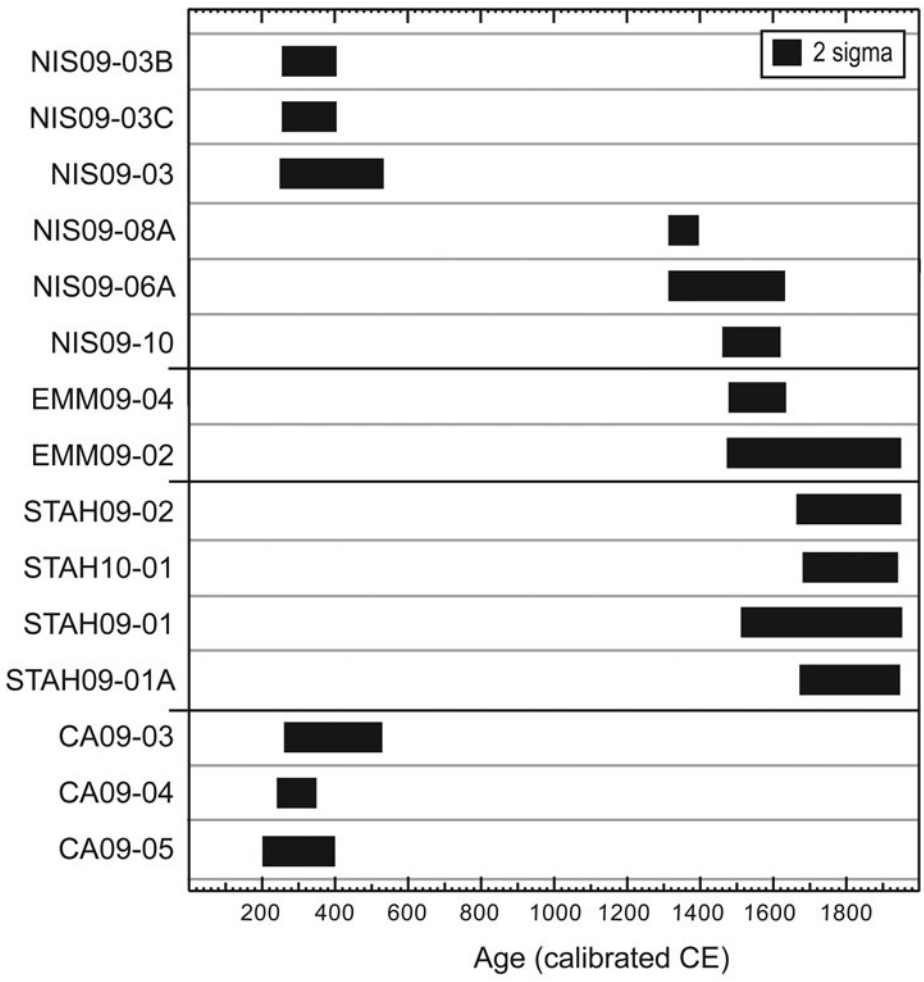

Figure 12. Distribution of radiocarbon ages of wood in lateral moraines and glacier forefields at Mount Rainier. Ages are calibrated with a standard error of 2 sigma. There are two clusters of ages, occurring in the first millennium and the second millennium CE, respectively. NIS = Nisqually Glacier, EMM = Emmons Glacier, STAH = South Tahoma Glacier, and CA = Carbon Glacier.

https://doi.org/10.1017/qua.2023.63 Published online by Cambridge University Press

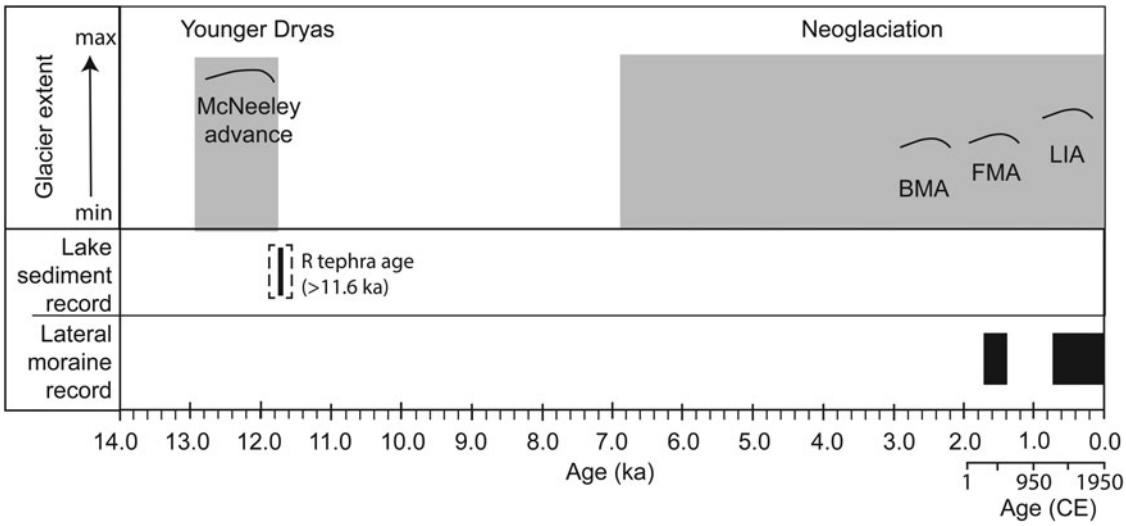

Figure 13. Schematic diagram of inferred glacier fluctuations on Mount Rainier over the past 14,000 years. A proposed timing of glacier advances is shown by curved black lines. Gray boxes show the Younger Dryas event and the Neoglacial period (Osborn et al., 2012). In the lake sediment record, the vertical black line inside the dashed rectangle indicates the position of the minimum-limiting age for R tephra (>11.6 ka) and the dashed rectangle shows a suggested period of paraglacial sedimentation, represented by clay sediments in the Tipsoo Lake sediment core, that post-dates the maximum extent of the McNeeley advance. In the lateral-moraine record, the black bars indicate the inferred timing on Mount Rainier of glacier advance during the First Millennium and Little Ice Age advances. BMA = Burroughs Mountain Advance; FMA = First Millennium Advance; LIA = Little Ice Age.

but do not capture the composite nature of many lateral moraines revealed by moraine stratigraphy. Our ages from paleosurfaces in tills add to dendrochronologic studies at Nisqually, Carbon, Emmons, and South Tahoma glaciers by Sigafoos and Hendricks (1972) and a lichenometric study at Carbon Glacier by Burbank (1981).

Interpretations at individual glaciers

Nisqually Glacier plastered till over a vegetated surface on the proximal moraine flank of its east lateral moraine sometime between 252 and 538 CE (Figs. 6, 10, and 12). The west lateral moraine of Nisqually Glacier contains several pieces of wood that were buried when till was deposited on the proximal moraine flank between 1308 and 1630 CE. About 700 m downvalley, Nisqually Glacier advanced and overtopped its moraine crest between 1457 and 1622 CE, when it reached at least ~1.6 km downvalley of its current position. Sigafoos and Hendricks (1972) dated an end moraine downvalley from our sample sites, with associated lateral moraines, and determined that the earliest LIA moraine stabilization occurred 1840 CE. Inner nested lateral moraines were also dated to 1857, 1870, and 1900 CE. The combined record indicates that Nisqually Glacier underwent Neoglacial advance starting as early as 250 CE and again as early as 1300 CE before eventually building the 1840 CE end moraine representing the maximum LIA advance. Nested lateral and recessional moraines from the nineteenth and twentieth centuries mark a period dominated by glacial retreat.

Carbon Glacier overtopped its west lateral moraine crest and buried a vegetated surface sometime between 205 and 529 CE (Figs. 8 and 12) during the first millennium CE. This record contrasts with the east-lateral record of Burbank (1981) who observed tephra layer C (ca. 2.2 ka; Table 1) in tills below the moraine crest and interpreted that tills older than 2.2 ka, potentially from the Burroughs Mountain advance, lie directly below LIA tills. This implies that pre-LIA tills dating to the first millennium CE, like those found at our site on the west lateral moraine, are missing from the east lateral moraine or were not distinguished from LIA tills. The different preservation of evidence in the nested moraines of Carbon Glacier points to the complexity of resolving the glacier fluctuation record using moraine stratigraphy. Sigafoos and Hendricks (1972) dated end and lateral moraines and determined that the oldest lateral-moraine set dates to 1500 CE with younger LIA nested moraine crests dating to 1835–1850 CE and 1875 CE. The combined record supports an advance of Carbon Glacier that is older than 2.2 ka as described by Burbank (1981), as well as periods of moraine building in the first millennium CE that culminated during the LIA as early as the sixteenth century. The culminating advance was followed by a dominantly recessional phase in which nested lateral moraines dating to the nineteenth century were built.

Emmons Glacier forefield contains several sets of nested lateral moraines. Our examination of these moraines indicates the glacier overtopped a west lateral moraine as early as the late 1400s (Figs. 7 and 12). Sigafoos and Hendricks (1972) dated lateral and end moraines downvalley from our study site and found that the oldest lateral-moraine crest dates to 1550 CE. This perhaps indicates that the late 1400s tills dated upvalley may be from the same advance that built the 1550 CE downvalley lateral moraine. Retreat from the end moraine that represents the maximum downvalley limit of Emmons Glacier was underway by the mid-1600s, and the glacier built several recessional end and lateral moraines during the eighteenth, nineteenth, and twentieth centuries (Sigafoos and Hendricks, 1972).

Wood fragments and sheared stumps in growth position are exposed in a wood mat on the north gully wall of Tahoma Creek, which has incised into the forefield of South Tahoma Glacier (Figs. 9, 10, and 12). Outer rings of a sheared stump (STAH10-01; 35 cm in diameter) in growth position date to between 1682 and 1939 CE and provide the tightest constraint on the age of the wood mat. The Tahoma Creek drainage is frequently inundated by lahars (Walder and Driedger, 1994, 1995), which have been known to 'shear' trees leaving behind stumps

https://doi.org/10.1017/qua.2023.63 Published online by Cambridge University Press

(J. Vallance, personal communication, 2010). But we attribute the shearing of the stumps, as large as 81 cm in diameter, in the wood mat to a glacier advance rather than a lahar.

The dated wood mat in the South Tahoma Glacier forefield is ~150 m upvalley from the oldest LIA end moraine and within the bounds of the lateral-moraine ridges that were dated dendrochronologically by Sigafoos and Hendricks (1972). The end moraines and their lateral moraines date to 1550, 1835–1850, and 1860 CE (Sigafoos and Hendricks, 1972; Fig. 9). Our radiocarbon ages, together with the age of the end moraines (Sigafoos and Hendricks, 1972), suggest that South Tahoma Glacier retreated at least 150 m upvalley after building its maximum LIA end moraine in 1550 CE, allowing trees to establish in the forefield, prior to a glacier re-advance into the vegetated forefield that sheared the stumps found in growth position in our wood mat as early as the late 1600s CE and later constructed the 1860 CE moraines.

Regional comparisons

Our record of calibrated radiocarbon ages of wood in lateral moraines and previous records employing dendrochronology, lichenometry, and tephrochronology (Crandell, 1969; Sigafoos and Hendricks, 1972; Crandell and Miller, 1974; Burbank, 1981) indicate that there were two intervals of glacier expansion on Mount Rainier in the late Neoglacial period (Figs. 12 and 13). The earlier event, evident in the lateral-moraine record of Nisqually and Carbon glaciers, was an advance between ca. 200 and 550 CE. The time of this event aligns well with that of the First Millennium Advance (FMA; Reyes et al., 2006), which is documented in several areas of the western North American Cordillera (Menounos et al., 2009), perhaps in response to the climatic cooling termed the Late Antique Little Ice Age (Büntgen et al., 2016). Evidence of this advance is not preserved in the end-moraine record on Mount Rainier; its end moraines were likely destroyed in more recent and extensive LIA advances of the last millennium. Our radiocarbon dating of the lateral-moraine stratigraphic record indicates that the LIA may have begun as early as ca. 1300 CE on Mount Rainier, aligning with the timing suggested in Clague et al. (2009).

CONCLUSIONS

Our work on Mount Rainier indicates (1) that valley glaciers on high Cascade volcanoes such as Mount Rainier are substantial and their advances extended into forest. In such environments, lateral-moraine stratigraphy can augment end-moraine dating in establishing glacial history. However, lateral moraines do not provide the same information: end-moraine ages fix culminations of glacier advances, whereas ages from paleosurfaces in lateral moraines help define the progress of advances toward their culminations and may bracket the timing of culminations. (2) At least some of the lateral moraines on Mount Rainier are composite features, built up by successive glacial advances, with LIA till at the crest, a till dated to the first millennium CE below that, and still older till(s) below that. (3) Moraine stratigraphy establishes two major episodes of Neoglacial advance. The first is a pre-LIA advance on Mount Rainier that was less extensive than LIA maximum advances and was previously undocumented in the Cascade Range. It occurred between 200 and 550 CE and corresponds to the First Millennium Advance in western Canada. The second episode began around 1300 CE and culminated in the LIA maximum advances. (4) The early Neoglacial Burroughs Mountain advance proposed by Crandell and Miller (1974) relies on ambiguous interpretations of tephra distribution. Although an early Neoglacial advance on Mt. Rainier is likely given records elsewhere in the Cordillera, evidence is scant at Mount Rainier. (5) A single episode of latest Pleistocene or Early Holocene ice advance on Mount Rainier is marked by the McNeeley moraines, as proposed by Crandell and Miller (1974). Our mapping counters a previous interpretation of two such advances by Heine (1997, 1998a). (6) Based on two additional radiocarbon ages from a sediment core from Tipsoo Lake, we revise the age estimate of R tephra to >11.6 ka, thereby making the McNeeley advance a possible consequence of the 12.9–11.7 ka Younger Dryas cold interval.

Supplementary Material. The supplementary material for this article can be found at https://doi.org/10.1017/qua.2023.63.

Acknowledgments. This research was supported by funding from the National Science and Engineering Research Council (NSERC) and the Canada Chairs Program, including NSERC Grant # 9026 to G. Osborn and M. Samolczyk. Funding was also provided by the University of Calgary and the Bentley University Faculty Research Awards. We are grateful for assistance provided by Joel Cubley, Jon Riedel, Eric Steig, Zoë Dietrich, Kristyn Adams, Randall Burke, Aline LaBrie, Josh Ouellet, Natalie Vogt, Jezra Beaulieu, Niki Clark, Nigel Davies, Dan Shugar, and Courtenay Brown. We would like to thank Brian Luckman, Greg Wiles, and James O'Connor for helpful reviews.

REFERENCES

Armstrong, J.E., Crandell, D.R., Easterbrook, D.J., 1965. Late Pleistocene stratigraphy and chronology in southwestern British Columbia and northwestern Washington. *GSA Bulletin* **76**, 321–330.

Bakke, J., Lie, Ø., Nesje, A, Svein, O.D., Dahl, S.O., Paasche, Ø., 2005. Utilizing physical sediment variability in glacier-fed lakes for continuous glacier reconstructions during the Holocene, northern Folgefonna, western Norway. *The Holocene* **15**, 161–176.

Barnekow, L., Possnert, G., Sandgren, P., 1998. AMS ^{14}C chronologies of Holocene lake sediments in the Abisko area, northern Sweden – a comparison between dated bulk sediment and macrofossil samples. *Journal of the Geological Society of Sweden* **120**, 59–67.

Beason, S.R., Kenyon, T.R., Jost, R.P., Walker, L.J., 2022, A vanishing landscape: current trends for the glaciers of Mount Rainier National Park, Washington, USA. *Geological Society of America Abstracts with Programs* **54**, no. 5. https://gsa.confex.com/gsa/2022AM/webprogram/Paper381984.html.

Bender, V., Haines, A.L., 1955. Forty-two years of recession of the Nisqually Glacier on Mount Rainier. *Erdkunde* **9**, 275–281.

Bilderback, E.L., 2004. *Timing and paleoclimatic significance of latest Pleistocene and Holocene cirque glaciation in the Enchantment Lakes Basin, North Cascades, Washington*. M.Sc. thesis, Western Washington University, Bellingham, WA, 39 pp.

Bowerman, N.D., Clark, D.H., 2011. Holocene glaciation of the central Sierra Nevada, California. *Quaternary Science Reviews* **30**, 1067–1085.

Brace, S., Peterson, D.L., 1998. Spatial patterns of tropospheric ozone in the Mount Rainier region of the Cascade Mountains, U.S.A. *Atmospheric Environment* **32**, 3629–3637.

Büntgen, U., Myglan, V., Ljungqvist, F., McCormick, M., Di Cosmo, N., Sigl, M., Jungclaus, J., *et al.*, 2016. Cooling and societal change during the Late Antique Little Ice Age from 536 to around 660 AD. *Nature Geoscience* **9**, 231–236.

Burbank, D.W., 1981. A chronology of Late Holocene glacier fluctuations on Mount Rainier, Washington. *Arctic and Alpine Research* **13**, 369–386.

Burbank, D.W., 1982. Correlations of climate, mass balances, and glacial fluctuations at Mount Rainier, Washington, U.S.A., since 1850. *Arctic and Alpine Research* **14**, 137–148.

Cambardella, C.A., Gajda, A.M., Doran, J.W., Wienhold, B.J., Kettler, T.A., 2001. Estimation of particulate and total organic matter by weight

loss-on-ignition. In: Lal, R., Kimble, J.M., Follett, R.F., Stewart, B.A. (Eds.), *Assessment Methods for Soil Carbon*. Lewis Publishers, New York, pp. 349–359.

Cheng, H., Zhang, H., Spotl, C., Edwards, R.L., 2020. Timing and structure of the Younger Dryas event and its underlying climate dynamics. *Proceedings of the National Academy of Sciences* **117**, 23408–23417.

Church, M., Ryder, J., 1972. Paraglacial sedimentation: a consideration of fluvial processes conditioned by glaciation. *Geological Society of America Bulletin* **83**, 3059–3072.

Clague, J., Menounos, B., Osborn, G., Luckman, B., Koch, J., 2009. Nomenclature and resolution in Holocene glacial chronologies. *Quaternary Science Reviews* **28**, 2231–2238.

Crandell, D.R., 1969. Surficial geology of Mount Rainier National Park, Washington. *U.S. Geological Survey Bulletin* **1288**, 41 pp.

Crandell, D.R., 1971. Postglacial lahars from Mount Rainier volcano, Washington. *U.S. Geological Survey Professional Paper* **677**, 75 pp.

Crandell, D.R., Miller, R.D., 1974. Quaternary stratigraphy and extent of glaciation in the Mount Rainier region, Washington. *U.S. Geological Survey Professional Paper* **847**, 59 pp.

Crandell, D.R., Mullineaux, D.R., Miller, R.D., Rubin, M., 1962. Pyroclastic deposits of recent age at Mount Rainier, Washington. *U.S. Geological Survey Professional Paper* **450-D**, D64–D68.

Crandell, D.R., Mullineaux, D.R., Rubin, M., Spiker, K., Kelley M.L., 1981. Radiocarbon dates from volcanic deposits at Mount St. Helens, Washington. *U.S. Geological Survey Open File Report* **81–844**, 14 pp.

Davis, P.T., Menounos, B., Osborn, G., 2009. Holocene and latest Pleistocene alpine glacier fluctuations: a global perspective. *Quaternary Science Reviews* **28**, 2021–2033.

Davis, P.T., Osborn, G., 1987. Age of pre-Neoglacial cirque moraines in the central North American Cordillera. *Géographie Physique et Quaternaire* **41**, 365–375.

Dusik, J., Leopold, M., Heckmann, T., Haas, F., Hilger, L., Morche, D., Neugirg, F., Becht, M., 2014. Influence of glacier advance on the development of the multipart Riffeltal rock glacier, central Austrian Alps. *Earth Surface Processes and Landforms* **40**, 965–980.

Egan, J., Staff, R., Blackford, J., 2015. A high-precision age estimate of the Holocene Plinian eruption of Mount Mazama, Oregon, USA. *The Holocene* **25**, 1054–1067.

Fiacco, R.J., Palais, J.M., Germani, M.S., Zelinski., G.A., Mayewski, P.A., 1993. Characteristics and possible source of a 1479 A.D. volcanic ash layer in a Greenland ice core. *Quaternary Research* **39**, 267–273.

Fiske, R.S., Hopson, C.A., Waters, A.C., 1963. Geology of Mount Rainier National Park, Washington. *U.S. Geological Survey Professional Paper* **444**, 93 pp.

Grimm, E., Nelson, D., 2009. The magnitude of error in bulk-sediment radiocarbon dates from central North America. *Quaternary Research* **72**, 301–308.

Heine, J.T., 1997. *Glacier advances at the Pleistocene/Holocene transition near Mount Rainier volcano, Cascade Range, USA*. Ph.D. thesis, University of Washington, Seattle, WA, 138 pp.

Heine, J.T., 1998a. Extent, timing, and climatic implications of glacier advances, Mount Rainier, Washington, U.S.A., at the Pleistocene/Holocene transition. *Quaternary Science Reviews* **17**, 1139–1148.

Heine, J.T., 1998b. A minimal lag time and continuous sedimentation in alpine lakes near Mount Rainier, Cascade Range, Washington, USA. *Journal of Paleoclimatology* **19**, 465–472.

Heiri, O., Lotter, A.F., Lemcke, G., 2001. Loss on ignition as a method for estimating organic and carbonate content in sediments: reproducibility and comparability of results. *Journal of Paleolimnology* **25**, 101–110.

Hobson, F.D., 1976. *Classification system for the soils of Mount Rainier National Park*. M.S. thesis, Washington State University, Pullman, WA, 79 pp.

Humlum, O., 1978. Genesis of layered lateral moraines: Implications for palaeoclimatology and lichenometry. *Geografisk Tidsskrift* **77**, 65–72.

Iturrizaga, L., 2008. Post-sedimentary transformation of lateral moraines – the tributary tongue basins of the Kviárjökull (Iceland). *Journal of Mountain Science* **5**, 1–16.

Karlén, W., 1976. Lacustrine sediments and tree-limit variations as indicators of Holocene climatic fluctuations in Lappland, northern Sweden. *Geografiska Annaler* **58**, 1–34.

Karlén, W., 1981. Lacustrine sediment studies: a technique to obtain a continuous record of Holocene glacier variations. *Geografiska Annaler* **63**, 273–281.

Karlén, W., Matthews, J.A., 1992. Reconstructing Holocene glacier variations from glacial lake sediments: studies from Nordvestlandet and Jostedalsbreen–Jotunheimen, southern Norway. *Geografiska Annaler* **74 (A)**, 327–348.

Kaufman, D., Porter, S., Gillespie, A., 2003, Quaternary alpine glaciation in Alaska, the Pacific Northwest, Sierra Nevada, and Hawaii. In: Gillespie, A., Porter, S., Atwater, B. (Eds.), *The Quaternary Period in the United States*. Elsevier Developments in Quaternary Sciences, vol. 1, pp. 77–103.

Kovanen, D.J., Beget, J.E., 2005. Comments on "Early Holocene glacier advance, southern Coast Mountains, British Columbia." *Quaternary Science Reviews* **24**, 1521–1525.

Leonard, E.M., Reasoner, M.A., 1999. A continuous Holocene glacial record inferred from proglacial lake sediments in Banff National Park, Alberta, Canada. *Quaternary Research* **51**, 1–13.

Livingston, D.A., 1955. A lightweight piston sampler for lake deposits. *Ecology* **36**, 137–139.

Loewenherz, D.S., Lawrence, C.J., Weaver, R.L., 1989. On the development of transverse ridges on rock glaciers. *Journal of Glaciology* **35**, 383–391.

Luckman, B.H., Holdsworth, G., Osborn, G.D., 1993. Neoglacial glacier fluctuations in the Canadian Rockies. *Quaternary Research* **39**, 144–155.

Matthes, F.E., 1928, Mount Rainier and its glaciers. U.S. National Park Service. https://www.nps.gov/parkhistory/online_books/mora/matthes/intro.htm.

Matthews, J.A., Petch, J.R., 1982. Within-valley asymmetry and related problems of Neoglacial lateral moraine development at certain Jotunheimen glaciers, southern Norway. *Boreas* **11**, 225–247.

Matthews, J.A., Svein, O.D., Nesje, A., Berrisford, M.S., Andersson, C., 2000. Holocene glacier variations in central Jotunheimen, southern Norway based on distal glaciolacustrine sediment cores. *Quaternary Science Reviews* **19**, 1625–1647.

Menounos, B., Clague, J. Gilbert, R., Slaymaker, O., 2005. Environmental reconstruction from a varve network in the southern Coast Mountains, British Columbia, Canada. *The Holocene* **15**, 1163–1171.

Menounos, B., Goehring, B., Osborn, G., Margold, M., Ward, B., Bond, J., Clarke, G., *et al.*, 2017. Cordilleran ice sheet mass loss preceded climate reversals near the Pleistocene termination. *Science* **358**, 781–784.

Menounos, B., Osborn, G., Clague, J., Luckman, B., 2009. Latest Pleistocene and Holocene glacier fluctuations in western Canada. *Quaternary Science Reviews* **28**, 2049–2074.

Mills, H.H., 1978. Some characteristics of glacial sediments on Mount Rainier, Washington. *Journal of Sedimentary Petrology* **48**, 1345–1356.

Mullineaux, D.R., 1974. Pumice and other pyroclastic deposits in Mount Rainier National Park, Washington. *U.S. Geological Survey Bulletin* **1326**, 83 pp.

National Park Service, 2018. Unpublished digital surficial geologic map of Mount Rainier National Park and vicinity, Washington (NPS, GRD, GRI, MORA, MORS digital map), adapted from a U.S. Geological Survey Bulletin map by Crandell (1969). http://datadiscoverystudio.org/geoportal/rest/metadata/item/1b4dbe6880d6492cb0322d8e696f197a/html. [accessed 8 January 2022]

National Park Service, 2021a. Mount Rainier National Park, Washington. *Frequently Asked Questions. Updated July* **6**, 2021. https://www.nps.gov/mora/faqs.htm. [accessed 11 August 2021]

National Park Service, 2021b. Mount Rainier National Park, Washington. *Weather. Updated September* **20**, 2021. https://www.nps.gov/mora/planyourvisit/weather.htm. [accessed 10 December 2021]

Nesje, A., Matthews, J.A., Dahl, S.O., Berrisford, M.S., Andersson, C., 2001. Holocene glacier fluctuations of Flatebreen and winter precipitation changes in the Jostedalsbreen region, western Norway, based on glaciolacustrine records. *The Holocene* **11**, 267–280.

Niklaus, T.R., Bonani, G., Suter, M., Wölfli, W., 1994. Systematic investigation of uncertainties in radiocarbon dating due to fluctuations in the calibration curve. *Nuclear Instruments and Methods in Physics Research* **B92**, 194–200.

Osborn, G.D., 1978. Fabric and origin of lateral moraines, Bethartoli Glacier, Garhwal Himalaya, India. *Journal of Glaciology* **20**, 547–553.

https://doi.org/10.1017/qua.2023.63 Published online by Cambridge University Press

Osborn, G., 1986. Lateral-moraine stratigraphy and Neoglacial history of Bugaboo Glacier, British Columbia. *Quaternary Research* **26**, 171–178.

Osborn, G., Karlstrom, E.T., 1989. Holocene moraine and paleosol stratigraphy, Bugaboo Glacier, British Columbia. *Boreas* **18**, 311–322.

Osborn, G.D., Robinson, B.J., Luckman, B.H., 2001. Holocene and latest Pleistocene fluctuations of Stutfield Glacier, Canadian Rockies. *Canadian Journal of Earth Sciences* **38**, 1141–1155.

Osborn, G., Menounos, B., Clague, J., Koch, J, Vallis, V., 2007. Multi-proxy record of Holocene glacial history of the Spearhead and Fitzsimmons ranges, southern Coast Mountains. *Quaternary Science Reviews* **26**, 479–493.

Osborn, G., Menounos, B., Riedel, J., Clague, J., Koch, J., Clark, D., Scott, K., Davis, P.T., 2012. Latest Pleistocene and Holocene glacier fluctuations on Mt. Baker, Washington, USA. *Quaternary Science Reviews* **49**, 33–51.

Porter, S.C., 1981. Lichenometric studies in the Cascade Range of Washington: establishment of *Rhizocarpon geographicum* growth curves at Mount Rainier. *Arctic and Alpine Research* **13**, 11–23.

Porter, S.C., Denton, G.H., 1967. Chronology of neoglaciation in the North American Cordillera. *American Journal of Science* **265**, 177–210.

Reimer, P.J., Austin, W.E.N., Bard, E., Bayliss, A., Blackwell, P.G., Bronk Ramsey, C., Butzin, M., *et al.*, 2020. The IntCal20 Northern Hemisphere radiocarbon age calibration curve (0–55 cal kBP). *Radiocarbon* **62**, 725–757.

Reyes, A.V., Wiles, G.C., Smith, D.J., Barclay, D.J., Allen, S., Jackson, S., Larocque, S., *et al.*, 2006. Expansion of alpine glaciers in Pacific North America in the first millennium A.D. *Geology* **34**, 56–60.

Riedel, J., Larrabee, M.A., 2011. *Mount Rainier National Park glacier mass balance monitoring annual report, water year 2009. North Coast and Cascades Network*. Natural Resource Technical Report NPS/NCCN/NRTR—2011/484. U.S. National Park Service, Fort Collins, CO. http://npshistory.com/publications/mora/nrtr-2011-484.pdf.

Rogers, G.C., 1985. Variation in Cascade volcanism with margin orientation. *Geology* **13**, 495–498.

Röthlisberger, F., Schneebeli, W., 1979. Genesis of lateral moraine complexes, demonstrated by fossil soils and trunks: indicators of postglacial climatic fluctuations. In: Schlüchter, C. (Ed.), *Moraines and Varves*. A.A. Balkema, Rotterdam, pp. 387–419.

Russell, I.C., 1898, Glaciers of Mt. Rainier. *U.S. Geological Survey,* 18th *Annual Report*, Part 2, pp. 355–409.

Ryder, J.M., Thomson, B., 1986. Neoglaciation in the southern Coast Mountains of British Columbia: chronology prior to the late-Neoglacial maximum. *Canadian Journal of Earth Sciences* **23**, 273–287.

Samolczyk, M., 2011. *Latest Pleistocene and Holocene glacier fluctuations in Mount Rainier National Park, Washington, USA*. M.Sc. thesis, University of Calgary, Calgary, AB, 153 pp.

Samolczyk, M.A., Vallance, J.W., Cubley, J.F., Osborn, G.D., Clark, D.H., 2016. Geochemical characterization and dating of R tephra, a postglacial marker bed in Mount Rainier National Park, Washington, USA. *Canadian Journal of Earth Sciences* **53**, 202–217.

Scott, K.M., Vallance, J.W., Pringle, P.T., 1995. Sedimentology, behaviour, and hazards of debris flows at Mount Rainier, Washington. *U.S. Geological Survey Professional Paper* **1547**, 56 pp.

Sigafoos, R.S. and Hendricks, E.L., 1961. Botanical evidence of the modern history of Nisqually Glacier, Washington. *U.S. Geological Survey Professional Paper* **387-A**, 20 pp.

Sigafoos, R.S, Hendricks, E.L., 1972. Recent activity of glaciers of Mount Rainier, Washington. *U.S. Geological Survey Professional Paper* **387-B**, 24 pp.

Sisson, T.W., Lanphere, M.A., 2008. Lava and ice – growth and eruptive style of Mount Rainier. In: Pringle, P.T. (Ed.), *Roadside geology of Mount Rainier National Park and vicinity*. Washington Division of Geology and Earth Resources Information Circular **107**, pp. 30–34.

Sisson, T.W., Vallance, J.W., 2009. Frequent eruptions of Mount Rainier over the last ~2,600 years. *Bulletin of Volcanology* **71**, 595–618.

Small, R.J., 1983. Lateral moraines of glacier Tsidjiore Nouve: form, development, and implications. *Journal of Glaciology* **29**, 250–259.

Smith, N.D., 1978. Sedimentation processes and patterns in a glacier-fed lake with low sediment input. *Canadian Journal of Earth Sciences* **15**, 741–756.

Stuiver, M., Reimer, P.J., Reimer, R.W., 2021. CALIB 8.2. http://calib.org. [accessed May 2021]

Swanson, D., 1993. *Variation in the grain size distribution and the chemical composition of the Mount Rainier C-ash unit*. BSc thesis, University of Puget Sound, Tacoma WA.

Thomas, P.A., Easterbrook, D.J., Clark, P.U., 2000. Early Holocene glaciation on Mount Baker, Washington State, USA. *Quaternary Science Reviews* **19**, 1043–1046.

U.S. Geological Survey, 2023. *The National Geologic Map Database*. https://ngmdb.usgs.gov/ngmdb/ngmdb_home.html. [accessed May 2023]

Vallance, J.W., 2000. Lahars. In: Sigurdsson, H. (Ed.), *Encyclopedia of Volcanoes*. Academic Press, pp. 601–616.

Vallance, J.W., Cunico, M.L., Schilling, S.P., 2003. Debris-flow hazards caused by hydrologic events at Mount Rainier, Washington. *U.S. Geological Survey Open-File Report* **03-368**, 10 pp.

Waitt, R.B., Yount, J.C., Davis, P.T., 1982. Regional significance of an early Holocene moraine in Enchantment Lakes Basin, North Cascade Range, Washington. *Quaternary Research* **17**, 191–210.

Walder, J.S., Driedger, C.L., 1994. Rapid geomorphic change caused by glacial floods and debris flows along Tahoma Creek, Mount Rainier, Washington, U.S.A. *Arctic and Alpine Research* **26**, 319–327.

Walder, J.S., Driedger, C.L., 1995. Frequent outburst floods from Tahoma Glacier, Mount Rainier, U.S.A.: relation to debris flows, meteorological origin and implications for subglacial hydrology. *Journal of Glaciology* **41**, 1–10.

Wright, H.E., Jr., 1967. A square-rod piston sampler for lake sediments. *Journal of Sedimentary Petrology* **37**, 975–976.

Wu, Y., Wang, S., Zhou, L., 2011. Possible factors causing older radiocarbon age for bulk organic matter in sediment from Daihai Lake, North China. *Radiocarbon* **53**, 359–366.

Yamaguchi, D.K., 1983. New tree-ring dates for recent eruptions of Mount St. Helens. *Quaternary Research* **20**, 246–250.

Zdanowicz, C.M., Zielinski, G.A., Germani, M.S., 1999. Mount Mazama eruption: calendrical age verified and atmospheric impact assessed. *Geology* **27**, 621–624.

https://doi.org/10.1017/qua.2023.63 Published online by Cambridge University Press